Egypt.J.Chem. **Vol. 63,** No. 3. pp. 1009-1031 (2020)

Egyptian Journal of Chemistry

http://ejchem.journals.ekb.eg/

Template Synthesis, Spectral and Thermal Properties of Nd(III) Metformin Schiff-Base Complexes As Potential Hypoglycemic Agents

M. A. Mahmoud[1*], Mahmoud G. Abou-elmagd [2]

[1]*Department of Science and Mathematics Engineering, Faculty of Petroleum and Mining Engineering, Suez University, Suez, Egypt*

[2]*Holding Company for Water & Wastewater, Ismailia, Egypt.*

ND(III) complexes with Schiff-bases obtained by condensation of metformin with each of salicylaldehyde (HL^1); 2,3- dihydroxybenzaldehyde (H_2L^2); 2,4-dihydroxybenzaldehyde (H_2L^3); 2,5- dihydroxybenzaldehyde (H_2L^4) and 3,4-dihydroxybenzaldehyde (H_2L^5); and 2-hydroxynaphthaldehyde (HL^6) have been synthesized using the template reaction. The complexes were characterized by elemental analysis, conductivity and magnetic moment measurements, IR, UV-Vis., emission, GC-MS and XRD spectroscopy and thermal analysis. The complexes are eight coordinated structure with formulae $[NdL^{1-4,6}(NO_3)_2(H_2O)_3].nH_2O$ where n = 2, 3, 3, 4, 5 and $[NdL^5(NO_3)(H_2O)_5].2H_2O$. The nitrate appears to coordinate in the monodentate fashion to the metal ion. The complexes have hexagonal bipyramide stereochemistry as shown by the UV-Vis spectra and molecular modeling calculations. The thermal stabilities of the complexes have been studied by TGA, DTG and DTA and Coats-Redfern method was used to calculate their kinetic parameters. The mechanism of thermal decomposition was suggested using IR spectra at different temperatures. The association constants (K_b) for the interaction of glucose with the complexes were calculated at physiologically relevant pH (phosphate buffer) using UV-Vis and fluorescence spectroscopy as well as viscosity measurements.

Keywords: Glucose sensor, Metformin Schiff-bases, Nd(III) complexes, Spectral and thermal properties.

Introduction

Metformin hydrochloride(MF.HCl), (N,N-dimethyl-imido- dicarbonimidic diamide hydrochloride) or 1,1- dimethylbiguanide, it has two imino(-C=NH) and one each of primary($-NH_2$), secondary(-NH). Tertiary($-N(CH_3)_2$) amino groups as donating centers. Metformin is a commonly prescribed agent for the treatment of type II diabetes, includes multiple beneficial effects including weight loss and lipid reduction in addition to lowering blood glucose levels [1, 2]. It is an oral hypoglycemic agent, which enhances insulin sensitivity and is not effective in the absence of insulin [3]. The crystal structures of N,N-dimethylbiguanidium oxalate monohydrate and N,N-dimethylbiguanidium sulfate monohydrate were studied to elucidate the possible mechanism of N,N-dimethylbiguanide interacting with glucose [4]. The structure-hypoglycemic activity relationship for amides and hydrazones of succinic acid compared to MF and glyclazide has been studied [5]. Metal complexes of V, Cr, Mn, Co, Ni, Cu, Zn [6]; Mn^{2+} [7]; Cu^{2+} [8]; Fe^{3+} [9], Zn, Pd, Pt [10]; Mn, Fe, Ni, Cu, Zn, Cd, Mg, Sr, Ba, Pt, Au, Pd [11]; and Cr^{3+} [12] with MF were prepared and characterized. Copper(II) complex derived from the condensation of MF with 2-pyridinecarbaldehyde was synthesized and its antibacterial activity was studied by Gao [13]. In addition, Ni(II) complexes with the MF and pentane-2,4-dione Schiff-base were synthesized and characterized [14]. MF Schiff-bases with each of hydroxy- and dihydroxybenzaldehyde have reacted with Cr(III) and VO^{2+} by template method and their complexes were found to have antidiabetic activity [15, 16]. On the other hand, the same Schiff-bases have reacted with Cu(II) and their complexes showed toxicity to alloxane induced-diabetic mice [17].

Coordination and bioinorganic chemistry of

*Corresponding author e-mail: marwaahmed7610@yahoo.com, 00201012515801
Received 21/6/2019; Accepted 15/8/2019
DOI: 10.21608/ejchem.2019.13640.1858
©2020 National Information and Documentation Center (NIDOC)

lanthanide complexes had acquired increasing interest due to their motivating structures. Variety of lanthanide complexes have been proven to be very good antibacterial, anti-inflammatory, antiviral, anticoagulant and antitumor agents owing to their special electronic configuration [18-23]. Among them, some of those containing Gd(III) are widely used in biomedical analysis as magnetic resonance imaging (MRI) contrast agents both for its high paramagnetism and favorable properties in terms of electronic relaxation [24]. Recently, we have prepared and characterized Pr^{3+} and Dy^{3+} with MF Schiff-bases and their interaction with glucose in neutral medium was evaluated [25, 26].

In continuation for our study to increase the ability of MF for glucose sensing, a series of neodymium complexes with Schiff-bases of MF with salicylaldehyde (HL^1); 2,3-dihydroxybenzaldehyde (H_2L^2); 2,4-dihydroxy-benzaldehyde (H_2L^3); 2,5-dihydroxybenzaldehyde (H_2L^4); 3,4-dihydroxybenzaldehyde (H_2L^5); and 2-hydroxynaphthaldehyde (HL^6) were synthesized by template reaction. The resulting complexes were characterized using elemental analysis, conductivity measurements, magnetic moment values, spectral analysis (UV–Vis, fluorescence, IR, GC-MS, XRD), TG, DTG and DTA and molecular modeling calculations. Also, we describe the utility of the Nd-metformin complexes towards the detection of glucose at physiologically relevant pH in phosphate buffer solution using UV-Vis and fluorescence spectra as well as viscosity measurements.

Experimental

Materials

All chemicals used for the preparation were of analytical reagent grade and were used without further purification. Salicylaldehyde, 2,3-dihydroxybenzaldehyde, 2,4-dihydroxybenzaldehyde, 2,5-dihydroxy-benzaldehyde, 3,4-dihydroxy-benzaldehyde and 2-hydroxynaphthaldehyde (Koch-light laboratories) were used directly. Metformin–HCl was received from El-Nasr Company for Pharmaceutical Chemicals, Cairo, Egypt. Nd(NO3)3.6H2O was obtained from Aldrich Chemical Company. Glucose was supplied by Sigma-Aldrich, St. Louis, Missouri, USA.

Synthesis of the Schiff-bases

The Schiff-bases have been prepared by the addition of methanolic MF.HCL solution with a methanolic solution of the aldehyde in 1:1 mole ratio in the basic medium [15]. The reaction mixture was stirred continuously and refluxed over water bath for two hours. The colour of the solution changed to yellow colour indicating the formation of the Schiff-base. Only, HL^1 Schiff-base was isolated in the solid state, dried under vacuum and recrystallized from methanol (m.p. 195°C). The same method was followed in preparation of the other Schiff-bases with different aldehydes but trials to obtain the solid compounds were unsuccessful.

Template synthesis of the complexes [25,26]

All complexes were prepared from the following general procedure. 0.438 g (1 mmol) of $Nd(NO_3)_3.6H_2O$ in 10 mL of methanol was added dropwise to 1 mmol methanolic solution of the Schiff-base obtained from the previous step. The resulting solution was refluxed on water bath for two hours with stirring during which a colored solution is formed (pH = 4–4.5), after which NH_4OH is added dropwise tell the complex is precipitated (pH = 6–7). Stirring is continued for another one hour at room temperature, the complex is filtered, washed thoroughly with water and hot methanol and dried under vacuum. The following series of complexes were obtained: $[NdL^1(NO_3)_2(H_2O)_3].2H_2O$, $[NdL^2(NO_3)_2(H_2O)_3].3H_2O$, $[NdL^3(NO_3)_2(H_2O)_3].3H_2O$, $[NdL^4(NO_3)_2(H_2O)_3].4H_2O$, $[NdL^5NO_3(H_2O)_5].2H_2O$ and $[NdL^6(NO_3)_2(H_2O)_3].5H_2O$.

Analytical and physical measurements

C, H, and N were estimated using a Heraus CHN-rapid analyzer. The IR spectra were recorded (KBr disc) in the 400–4000 cm^{-1} range on Bruker Vector-22 spectrometer. The electronic absorption spectra were obtained by 10^{-3}M DMSO solution in 1cm quartz cell using Shimadzu UV-1800 double beam photometric system. Fluorescence spectra were performed on JASCO FP-6300 spectrofluorometer using quartz cell type 111-QS with a 150W xenon lamp for excitation. X-ray powder diffraction was performed using a Brucker Axs-D8 advance diffractometer with Cu-Kα radiation. GC-MS spectra were obtained using Shimadzu Qp-2010 Plus with EI ionization mode and electron voltage 70eV. Magnetic susceptibility measurements were carried out using the modified Gouy method [27] on MSB-MK1 balance at room temperature using mercury(II)tetrathiocyanatecobaltate(II) as a standard. The effective magnetic moment,

μ_{eff}, per metal atom was calculated from the expression μ_{eff}= 2.83√(χ.T) B.M, where χ is the molar susceptibility corrected using Pascal's constant for the diamagnetism of all atoms in the complexes. TGA, DTG and DTA were recorded on Shimadzu H-60 thermal analyzer under a dynamic flow of nitrogen (30 ml/min.) and heating rate 10°C/min. from ambient temperature to 750 or 1000°C. Electrical conductivity measurements were carried out at room temperature on freshly prepared 10^{-3}M DMF solutions using WTW conductivity meter fitted with L100 conductivity cell. Metal content was obtained by EDTA titration using xylenol orange as an indicator using acetate buffer.

Results and Discussion

Ligand characterization

MF.HCL react with aldehyde (1:1 mole ratio) in basic methanol medium (NaOH, CH_3COONa or aqueous NH_3) to give the Schiff-bases [15]. The mixture was refluxed with continuous stirring over water bath for two hours. The solution turns to yellow colour indicating Schiff-base formation. TLC in methanol-chloroform solvent mixture (1:10 v/v) was used to check the purity of the compounds. The compounds have been characterized using C, H, N analysis, ^{1}H NMR, UV–Vis and GC-MS spectra as well as TGA, DTG and DTA analysis. HL^1 structure is shown in Structure 1.

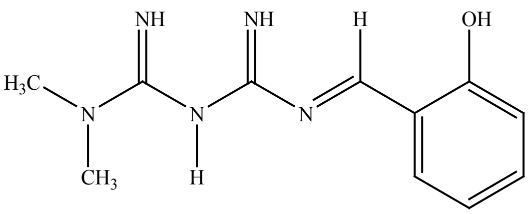

Structure 1. HL^1 Schiff-base.

Neodymium(III) complexes

Template reaction method was used to prepare series of Nd^{3+} complexes with Schiff-bases of MF with salicylaldehyde (HL^1); 2,3-dihydroxybenzaldehyde (H_2L^2); 2,4-dihydroxybenzaldehyde (H_2L^3); 2,5-dihydroxybenzaldehyde (H_2L^4) and 3,4-dihydroxybenzaldehyde (H_2L^5) and 2-hydroxynaphthaldehyde (HL^6) in methanol medium under reflux. The physical and analytical data of the complexes are summarized in Table 1. The elemental analysis of the new complexes suggests the following molecular formulas: $[NdL^{1-4,6}(NO_3)_2(H_2O)_3].nH_2O$ where n = 2, 3, 3, 4, 5 and $[NdL^5(NO_3)(H_2O)_5].2H_2O$. All complexes were stable in air, decomposed at > 300°C (Table 1) and soluble in Lewis bases (DMF and DMSO). The nonelectrolytic character of these complexes is supported by the molar conductance values (35.4–7.0 $ohm^{-1}cm^2mol^{-1}$) of 10^{-3} M DMF solutions at 25°C [28].

Attempts to get crystals suitable for single-crystal studies were not obtained although the complexes are soluble DMSO and DMF. The X-ray powder diffraction patterns for the complexes were scanned in the 5-75^0 at λ=1.540598Å are shown in Fig. 1. From the patterns, it is evident that the complexes are amorphous.

IR spectra

Table 2 gives assignments of the most important IR bands of the Nd(III) complexes which have been made by comparing with the bands of HL^1 ligand and structurally similar molecules (Table 2 and Fig. S1 in supplementary file). The most significant bands of biguanide and Schiff- base moieties were observed in the major IR spectral features of the presented complexes. The Schiff-base showed a strong broad band ascribed to υ(OH) at 3456 cm^{-1} which disappeared in the spectra of Nd(III) complexes. This behavior indicated the deprotonation and coordination of the OH group. The hydrated complexes have OH-stretching frequencies as a broad band in the 3590-3536 and 3449-3426 cm^{-1} regions. Except for the complex $[NdL^5(NO_3)(H_2O)_5].2H_2O$, IR spectra of all the complexes show broad intense band in the 3392-3357 and 3219-3204 cm^{-1} due to the asym. and sym. stretching vibration of the N–H group . IR spectra of some complexes with biguanide Schiff-bases displayed these bands [14,29]. υ(C=N) bands for the complexes $[NdL^2(NO_3)_2(H_2O)_3].3H_2O$, $[NdL^3(NO_3)_2(H_2O)_3].3H_2O$, $[NdL^4(NO_3)_2(H_2O)_3].4H_2O$ and $[NdL^6(NO_3)_2(H_2O)_3]. 5H_2O$ were recorded as strong split bands at the 1641-1622 and 1590-1572 cm^{-1}, respectively [30]. The complex $[NdL^1(NO_3)_2(H_2O)_3].2H_2O$ exhibited the same band as strong frequency at 1629 cm^{-1} [30]. N–C–N stretching band appears in the 1546-1532 cm^{-1} interval. The possible bonding modes of the nitrate group was obtained from the infrared spectra. The coordinated nitrate bands υ(N=O) ($υ_5$), $υ_{as}(NO_2)$ ($υ_2$) and $υ_s(NO_2)$ ($υ_1$) were observed in the 1451-1410, 1388-1319 and 1041-1034 cm^{-1} region. Differentiation between mono and bidentate chelating nitrate depends on the separation $Δυ = υ_5 – υ_1$. As Δυ Increasing, the coordination changes from mono to bidentate and/or bridging modes. Δυ values for the complexes (Table 2) indicate monodentate nitrate (136-103 cm^{-1}) [31]. υ(C–O) is recorded as a medium band in the 1221-1184 cm^{-1} region confirming deprotonation and coordination of the phenolic oxygen to the neodymium ion. Medium bands in the 585-490 and 524-438 cm^{-1} range are assigned to υ(Nd-O) and υ(Nd-N) vibrations. The band υ(Ln-O) are usually broad and stronger ocurring at a higher frequency than υ(Ln-N) due to large dipole moment change in the vibration of Ln-O band compared to the Ln-N band [32, 33].

υ(NH) and υ(C=N) are manifested at 3360,3225 and 1637, 1572 cm^{-1} for the complex $[NdL^5NO_3(H_2O)_5].2H_2O$. These band frequencies are similar in number and position to the free HL^1 Schiff-base values and are different from the rest of the complexes which indicates the non-participation of either C=NH or HC=N groups in bonding. Also, N-C-N is absent in the IR spectrum of this complex. υ(N=O) ($υ_5$), $υ_{as}(NO_2)$ ($υ_2$) and $υ_s(NO_2)$ ($υ_1$) were detected at 1486, 1388 and 1039 cm^{-1} of the coordinated nitrate. Δυ value for this complex (98 cm^{-1}) is indicative of a monodentate nitrate (Table 2) [30]. Also, in this complex, υ(C–O) appears as a very strong band at 1292 cm^{-1} while the other complexes show this band with different values and shapes. A newly formed band at 596 cm^{-1} in the spectra of the complex is assigned to υ(Nd-O) [34]. Also, Nd^{3+} is a hard acid, so it is expected to prefer bonding through the two oxygen atoms of the hydroxyl groups (hard base) of the Schiff-base after deprotonation forming five membered rings which may be more stable than forming six membered rings through nitrogen atoms [35].

TABLE 1. Analytical data and conductivity measurements of the Nd^{3+} complexes of the metformin Schiff-bases.

Compound	Mol.wt.	Formula m/z	Yield %	Color	Decmp. Point(°C)	Elemental analysis Found (Calculated %) C	H	N	M	$_M\Omega^*$ DMF
$[NdL^1(NO_3)_2(H_2O)_3].2H_2O$	590.45	590.1	45	Greenish yellow	300>	22.6 22.3	4.2 4.0	16.9 16.6	24.9 24.4	7.0
$[NdL^2(NO_3)_2(H_2O)_3].3H_2O$	624.45	622.0	40	Dark army green	300>	21.2 21.1	4.3 4.1	15.3 15.7	23.4 23.0	7.5
$[NdL^3(NO_3)_2(H_2O)_3].3H_2O$	624.45	624.1	40	Crimson red	300>	21.5 21.1	4.2 4.1	15.5 15.7	23.3 23.0	7.3
$[NdL^4(NO_3)_2(H_2O)_3].4H_2O$	642.45	643.1	45	Black	300>	20.4 20.5	4.2 4.3	15.5 15.2	22.0 22.4	4.3
$[NdL^5NO_3(H_2O)_5].2H_2O$	579.51	578.8	46	Greenish yellow	300>	22.6 22.7	4.7 4.6	14.5 14.4	24.9 24.8	35.4
$[NdL^6(NO_3)_2(H_2O)_3].5H_2O$	659.51	658.0	45	Dark grey	300>	27.5 27.3	4.9 4.8	14.5 14.8	21.7 21.8	9.2

*Conductance of 10^{-3}M ($ohm^{-1}cm^2mol^{-1}$)

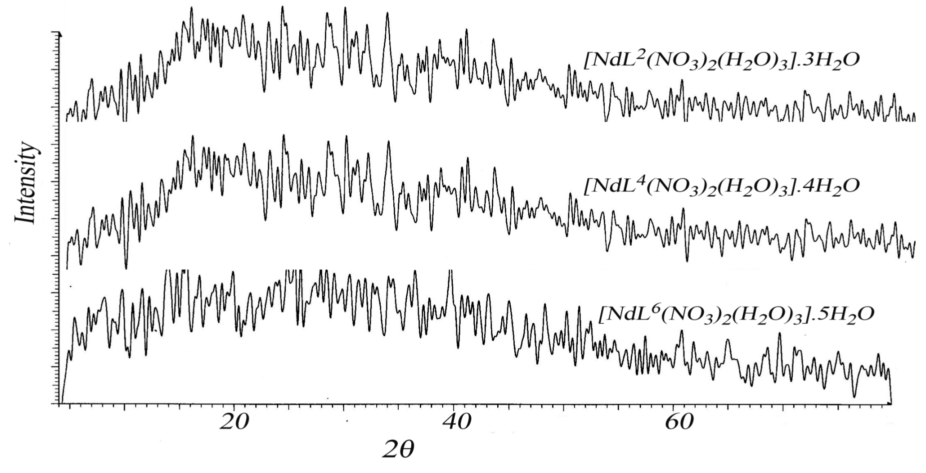

Fig. 1. XRD of the Nd^{3+} complexes of the metformin Schiff-bases.

TABLE 2. IR spectral data of the Nd^{3+} complexes of the metformin Schiff-bases.

Compound	(υH_2O) υ(OH)	υ(NH)	υ(C=N)	υ(N-C-N)	υ(C-O)	NO_3^- υ_5	NO_3^- υ_2	NO_3^- υ_1	$\Delta\upsilon$	υ(Nd-O) υ(Nd-N)
$[NdL^1(NO_3)_2(H_2O)_3].2H_2O$	3449 m.br.	3204 sh.	1629 s.	1532 m.	1186 m.	1439 s.	1319 s.	1034 m.	120	585 m. 473 m.
$[NdL^2(NO_3)_2(H_2O)_3].3H_2O$	3581 br. 3438 m.br.	3392 m. 3204 sh.	1629 s. 1589	1538 m.	1203 s.	1436 s.	1331 m.	1038 m.	105	567 m. 524 m.
$[NdL^3(NO_3)_2(H_2O)_3].3H_2O$	3580 br. 3440 m.br.	3371m.br. 3219 sh.	1615 s. 1580	1540 sh.	1221 m.	1410 m.	1307 m.	1037 m.	103	566 m. 515 m.
$[NdL^4(NO_3)_2(H_2O)_3].4H_2O$	3536 br. 3428 s.br.	3377 m. 3204 sh.	1641 s. 1590	1546 m.	1213 m.	1451 m.	1315m.	1041m.	136	495 m. 438 m.
$[NdL^5NO_3(H_2O)_5].2H_2O$	3590 br. 3426 m.br	3360 br. 3225 br.	1637 s. 1572	—	1292 vs.	1486 s.	1388 m.	1039 m.	98	596 m.
$[NdL^6(NO_3)_2(H_2O)_3].5H_2O$	3430 m.br.	3357 m. 3204 sh.	1622 s. 1587	1537 m.	1184 m.	1423 m.	1301 m.	1039 m.	122	490 m. 452 m.

s.=strong, vs.=very strong, m.=medium, br.=broad, sh.=shoulder, w.=weak.

Magnetic moment and spectral properties

The magnetic moment values for the neodymium(III) complexes lie in the range of 3.77–3.70 (Table 3). These values show little deviation from van Vleck values and those of hydrated nitrates [36].

Electronic structure of Nd^{3+} has the outer configuration $4f^3 5s^2 5p^6$ and follows the L, S, J coupling scheme but with a certain amount of configuration interaction. The 5s and 5p subshells have a radial dispersion which partially shield 4f electrons from the effect of coordinated ligands to a very large extent [37]. Thus, the electronic spectra of neodymium(III) can be considered as derived from the spectra of gaseous ions by a fairly small perturbation (nephelauxetic and crystal field splitting effects) [38–40]. The f^3 configuration of a free neodymium(III) ion involves 41 energy levels. The absorption spectra of neodymium(III) complexes contain many bands due to transitions from the ground level $^4I_{9/2}$ to exciting levels of the f^3 configuration. The absorption spectra of neodymium(III) complexes with metformin Schiff-bases show bands around 554-529, 610-580, 668-633, 679, 759-735, 796-848, and 868 nm corresponding to the transitions from the ground level $^4I_{9/2}$ to excited levels $^4G_{7/2}$, $^4G_{5/2}$, $^2H_{11/2}$, $^4F_{9/2}$, $^4F_{7/2}$, $^4F_{5/2}$ and $^4F_{3/2}$, respectively (Figs. S2-S4). The shapes of hypersensitive transitions of the complexes closely resemble that of the eight coordinated complexes [41].

Nephelauxetic effect is a shift of absorption bands towards lower energy on complex formation which is a general feature in the spectra of lanthanides [42]. This effect is described quantitatively by naphelauxetic parameter ($\bar{\beta}$) which is the ratio of the interelectronic repulsion parameter (either Slater's integrals F_k or Racah's parameter E^k) in the complex and in the free ion:

$\bar{\beta} = (F_k)$complex/((F_k)free ion) or

$\bar{\beta} = (E^k)$complex/((E^k)free ion)

The naphelauxetic effect value ($1-\bar{\beta}$) is small in lanthanide complexes, it can be defined from the ratio of the wavenumbers of f–f transitions in the spectra of the complex and the free ion:

$\bar{\beta} \approx \upsilon\_complex/\upsilon\_(free\ ion)$

The relative nephelauxetic effect values $\bar{\beta}$ are usually determined from experimental data using the spectra of the lanthanide aqua ions as standards:

$$\bar{\beta} = \frac{1}{n} \sum_{n=1}^{n} \frac{\upsilon_{complex}}{\upsilon_{aqua}}$$

From the mean $\bar{\beta}$ values, Sinha's covalency parameter (δ) and bonding parameter ($b^{½}$) are calculated using the following formulas [43].

$\delta = (1-\bar{\beta})/\bar{\beta} \times 100$ and $b^{½} = \sqrt{(1-\bar{\beta})/2}$

These parameters measure covalency which is the amount of 4f–ligand mixing. The values of the parameters β, δ and $b^{½}$ for the complexes are given in Table 3. The values of $\bar{\beta}$ being less than unity and the positive values of δ and $b^{½}$ support the partial covalent nature of bonding between metal and ligand [44, 45].

TABLE 3. UV-Vis spectra* of the Nd^{3+} complexes of the metformin Schiff-bases.

Compound	UV Bands(nm)	Assignment	$\xi*10^3$ $M^{-1}.cm^{-1}$	Covalence parameters
Nd^{3+} free ion (aq.)	523	${}^4I_{9/2} \rightarrow {}^4G_{7/2}$	—	—
	576	${}^4I_{9/2} \rightarrow {}^2G_{7/2}$		
	582	${}^4I_{9/2} \rightarrow {}^4G_{5/2}$		
	623	${}^4I_{9/2} \rightarrow {}^2H_{11/2}$		
	673	${}^4I_{9/2} \rightarrow {}^4F_{9/2}$		
	742	${}^4I_{9/2} \rightarrow {}^4F_{7/2}$		
	795	${}^4I_{9/2} \rightarrow {}^4F_{5/2}$		
	867	${}^4I_{9/2} \rightarrow {}^4F_{3/2}$		
$[NdL^1(NO_3)_2(H_2O)_3].2H_2O$	264	$\pi \rightarrow \pi^*$	2.984	β_{avg} =0.9938
	320	$n \rightarrow \pi^*$	4.215	$b^{½}$= 0.03932
	580	${}^4I_{9/2} \rightarrow {}^4G_{5/2}$	0.03	δ=0.6224
	633	${}^4I_{9/2} \rightarrow {}^2H_{11/2}$	0.012	η= 0.0031
	679	${}^4I_{9/2} \rightarrow {}^4F_{9/2}$	0.0118	
	745	${}^4I_{9/2} \rightarrow {}^4F_{7/2}$	0.0175	
$[NdL^2(NO_3)_2(H_2O)_3].3H_2O$	267,301	$\pi \rightarrow \pi^*$	0.868	β_{avg} =0.9865
	331	$n \rightarrow \pi^*$	2.723	$b^{½}$= 0.0579
	590	${}^4I_{9/2} \rightarrow {}^4G_{5/2}$	2.8	δ=1.3610
	652	${}^4I_{9/2} \rightarrow {}^2H_{11/2}$	2.8	η= 0.00678
	747	${}^4I_{9/2} \rightarrow {}^4F_{7/2}$	2.71	
	796	${}^4I_{9/2} \rightarrow {}^4F_{5/2}$	2.66	
	868	${}^4I_{9/2} \rightarrow {}^4F_{3/2}$	2.62	
$[NdL^3(NO_3)_2(H_2O)_3].3H_2O$	281	$\pi \rightarrow \pi^*$	0.178	β_{avg} =0.9608
	322	$n \rightarrow \pi^*$	0.178	$b^{½}$= 0.0989
	554	${}^4I_{15/2} \rightarrow {}^4G_{7/2}$	3.18	δ=4.077
	759	${}^4I_{9/2} \rightarrow {}^4F_{7/2}$	3.04	η= 0.01004
$[NdL^4(NO_3)_2(H_2O)_3].4H_2O$	222,303	$\pi \rightarrow \pi^*$	0.241,0.037	β_{avg} =0.9584
	350	$n \rightarrow \pi^*$	2.066	$b^{½}$=0.1019
	610	${}^4I_{9/2} \rightarrow {}^4G_{5/2}$	2.30	δ=4.336
	668	${}^4I_{9/2} \rightarrow {}^2H_{11/2}$	2.28	η= 0.02145
	735	${}^4I_{9/2} \rightarrow {}^4F_{7/2}$	2.18	
	848	${}^4I_{9/2} \rightarrow {}^4F_{5/2}$	2.25	
$[NdL^5NO_3(H_2O)_5].2H_2O$	267	$\pi \rightarrow \pi^*$	0.722	β_{avg} =0.9916
	333	$n \rightarrow \pi^*$	5.75	$b^{½}$= 0.0456
	529	${}^4I_{9/2} \rightarrow {}^4G_{7/2}$	0.1463	δ=0.84223
	746	${}^4I_{9/2} \rightarrow {}^4F_{7/2}$	0.0507	η= 0.0042
$[NdL^6(NO_3)_2(H_2O)_3].5H_2O$	283	$\pi \rightarrow \pi^*$	4.29	β_{avg} =0.9799
	361	$n \rightarrow \pi^*$	3.71	$b^{½}$= 0.0708
	590	${}^4I_{9/2} \rightarrow {}^4G_{5/2}$	0.384	δ=2.0471
	640	${}^4I_{9/2} \rightarrow {}^2H_{11/2}$	0.25	η= 0.01018

*10^{-3}M in DMSO

Emission Spectra

Trivalent lanthanides have specific luminescence properties due to the 4f electrons that are shielded from the environment by the filled 5s and 5p shells. As a result, the emission bands due to the intraconfigurational 4f→4f transitions are hardly influenced by the lanthanide ion′s surroundings, and therefore occur always at more or less the same wavelength. Another consequence of this shielding is the narrow line-like the appearance of the emission bands, giving rise to a high color-purity. However, because of the forbidden nature of the 4f-4f transitions, trivalent lanthanides have very low molar absorptivities, typically lower than 10, and often even less than 1 $L.mol^{-1}.cm^{-1}$, which makes them hard to excite. In coordination chemistry, a way to circumvent this problem is to make complexes with lanthanides using organic ligands, preferably bearing extended delocalized π-systems. These ligands serve as antennas, absorbing a large amount of light, and, if the energy levels match well with the lanthanide′s energy levels, this energy can be passed on to the lanthanide, which then emits it as light with its specific wavelength(s) [18].

At room temperature, complexes of the Nd-Schiff bases exhibited emission spectra in the UV-Vis region. These photophysical properties are summarized in Table 4. The steady-state UV-Vis emission spectra of the complexes in DMF solutions at a concentration of 10^{-5} M were carried out (Figs. S5-S7 in supplementary file). In these conditions, excited electrons relax from the highest to the lowest excited states before they recombine radiatively or non-radiatively. It can be seen from Table 4 that the Nd(III) complexes of the metformin Schiff bases show strong emission when excited with 262, 358, and 359 nm radiation. They represent intraconfigurational transitions from the Nd^{3+} ion′s higher lying electronic energy levels to electronic ground state $^4I_{9/2}$. The following transitions were recorded: $^2G_{7/2}\rightarrow{}^4I_{9/2}$ at 522 and 570 nm; $^2H_{11/2}\rightarrow{}^4I_{9/2}$ at 633-620 nm; $^4F_{9/2}\rightarrow{}^4I_{9/2}$ at 690-675 nm; $^4F_{7/2}\rightarrow{}^4I_{9/2}$ at 752 nm; $^4S_{3/2}\rightarrow{}^4I_{9/2}$ at 740 and 753 nm; and finally $^4F_{5/2}\rightarrow{}^4I_{9/2}$ at 840-792 nm, respectively.

Mass spectra

Mass spectroscopy, which is mainly applied in the analysis of biomolecules has been increasingly used as a powerful structural characterization technique in coordination chemistry. The suggested structure of the Nd^{3+} complexes was confirmed from the GC-MS spectra (Figs. S8-S10 in supplementary file). The peaks related to the molar masses of the complexes and its structural fragments based on Nd isotopes 142-150 are listed in Table 5. The spectra of ^{142}Nd isotope show fragments assignable to $[M]^+$ and $[M+1]^+$ by the complexes $[NdL^2(NO_3)_2(H_2O)_3].3H_2O$ and $[NdL^1(NO_3)_2(H_2O)_3].2H_2O$, $[NdL^5(NO_3)(H_2O)_5].2H_2O$, $[NdL^6(NO_3)_2(H_2O)_3].5H_2O$ at m/z (calcd./found %): 622.27/ 622.0% and 588.27/ 589.1%, 577.27/ 578.8%, 657.27/ 658.3%, respectively. Only the complex $[NdL^5(NO_3)(H_2O)_5].2H_2O$ shows the molecular ion peak $[M]^+$ for ^{143}Nd at m/z=578.27/578.8%. Also, ^{144}Nd and ^{145}Nd isotopes of the complexes $[NdL^1(NO_3)_2(H_2O)_3].2H_2O$, $[NdL^3(NO_3)_2(H_2O)_3].3H_2O$ and $[NdL^3(NO_3)_2(H_2O)_3].3H_2O$,$[NdL^4(NO_3)_2(H_2O)_3].4H_2O$ indicated the $[M]^+$ ion peak at m/z (calcd./found%): 590.27/590.1%, 624.27/624.1% and 625.27/ 625.1%, 643.27/643.1%, respectively. $[M]^+$ fragment of the ^{146}Nd and ^{148}Nd isotopes are seen by the spectra of the complexes $[NdL^1(NO_3)_2(H_2O)_3].2H_2O$ and $[NdL^3(NO_3)_2(H_2O)_3].3H_2O$ while $[M+1]^+$ fragment of the same isotopes are shown in the spectra of $[NdL^2(NO_3)_2(H_2O)_3].3H_2O$, $[NdL^5(NO_3)(H_2O)_5].2H_2O$ and $[NdL^4(NO_3)_2(H_2O)_3].4H_2O$, $[NdL^6(NO_3)_2(H_2O)_3].5H_2O$, respectively. Finally, the complex $[NdL^4(NO_3)_2(H_2O)_3].4H_2O$ indicates the molecular ion peak for the ^{150}Nd at m/z (calcd./found%): 648.27/648.1% refereing to $[M]^+$ fragment of the complex suggesting the monomeric nature of the complex and confirms the proposed formula.

Thermal analysis

The thermal behavior of some selected metal complexes was characterized on the basis of TGA, DTG and DTA methods in the 30-750°C range except the complexes $[NdL^1(NO_3)_2(H_2O)_3].2H_2O$, $[NdL^3(NO_3)_2(H_2O)_3].3H_2O$ and $[NdL^5NO_3(H_2O)_5].2H_2O$ in the 30-1000°C region. Thermoanalytical data of the complexes are given in Tables 6 and 7; the TG/DTA thermograms of the complex and , as representative examples, are represented in Fig. 2.

From this table, it is clear that all the metal complexes –except $[NdL^5NO_3(H_2O)_5].2H_2O$ which decomposes in four steps–underwent thermal decomposition within three steps. The first step for the complexes $[NdL^2(NO_3)_2(H_2O)_3].3H_2O$, $[NdL^3(NO_3)_2(H_2O)_3].3H_2O$, $[NdL^4(NO_3)_2(H_2O)_3].4H_2O$, $[NdL^5NO_3(H_2O)_5].2H_2O$ and $[NdL^6(NO_3)_2(H_2O)_3].5H_2O$ occurred within the range 20-196, 35-118, 19-203, 33-222 and 18-153°C with DTG_{max} at 73, 73, 76, 70 and 72°C, respectively, correspond to the loss of 3, 3, 4, 2 and 5 molecules crystallization water. Mass reduction observed during this step is (found/calcd.): 8.5/8.64%, 8.8/8.64%, 11.5/11.2%, 6.75/6.21% and 13.41/13.64% associated with endothermic changes with DTA_{max} at 77, 78, 82, 75 and 76°C. Also, in the first step, the complex $[NdL^1(NO_3)_2(H_2O)_3].2H_2O$ loses its hydration water in two steps. It is shown on the TG curve in the 26-191 range with DTG_{max} at 71 and 143°C. Total mass lowering observed was 6.52% against the calculated value of 6.09% denoting loss of two water molecules accompanied by endothermic

DTA_{max} at 73 and 143°C. This behavior shows that the complex contains two hydrated water molecules, one of them is strongly bonded to the crystal structure (143°C) and the other is weakly attracted (71°C). Enthalpy of dehydration was calculated to be in the 0.675-1.932 kJ/mol range.

TABLE 4. Fluorescence spectra and magnetic moment of the Nd^{3+} complexes of the metformin Schiff-bases.

Complex	λ_{ex}	λ_{em}	*RLI	Assignment	**μ_{eff} (B.M.)
$[NdL^1(NO_3)_2(H_2O)_3].2H_2O$	262	570 675 810	38 37 25	$^2G_{7/2}\rightarrow{}^4I_{9/2}$ $^4F_{9/2}\rightarrow{}^4I_{9/2}$ $^4F_{5/2}\rightarrow{}^4I_{9/2}$	3.75
$[NdL^2(NO_3)_2(H_2O)_3].3H_2O$	358	740 792	58 94	$^4S_{3/2}\rightarrow{}^4I_{9/2}$ $^4F_{5/2}\rightarrow{}^4I_{9/2}$	3.71
$[NdL^3(NO_3)_2(H_2O)_3].3H_2O$	359	690 752 800	38 53 48	$^4F_{9/2}\rightarrow{}^4I_{9/2}$ $^4F_{7/2}\rightarrow{}^4I_{9/2}$ $^4F_{5/2}\rightarrow{}^4I_{9/2}$	3.72
$[NdL^4(NO_3)_2(H_2O)_3].4H_2O$	359	620 680 840	160 160 100	$^2H_{11/2}\rightarrow{}^4I_{9/2}$ $^4F_{9/2}\rightarrow{}^4I_{9/2}$ $^4F_{5/2}\rightarrow{}^4I_{9/2}$	3.70
$[NdL^5NO_3(H_2O)_5].2H_2O$	359	633 680 753 816	23 32 27 22	$^2H_{11/2}\rightarrow{}^4I_{9/2}$ $^4F_{9/2}\rightarrow{}^4I_{9/2}$ $^4S_{3/2}\rightarrow{}^4I_{9/2}$ $^4F_{5/2}\rightarrow{}^4I_{9/2}$	3.72
$[NdL^6(NO_3)_2(H_2O)_3].5H_2O$	359	522 630 800	20 30 22	$^4G_{7/2}\rightarrow{}^4I_{9/2}$ $^2H_{11/2}\rightarrow{}^4I_{9/2}$ $^4F_{5/2}\rightarrow{}^4I_{9/2}$	3.77

*Relative luminescence intensity.
**Room temperature.

TABLE 5. Mass fragmentation of the Nd^{3+} complexes of the metformin Schiff-bases.

Complex	Nd isotope	m/z Calcd. (Found)	Abs. Int.	Rel. Int.	Assignment
$[NdL^1(NO_3)_2(H_2O)_3].2H_2O$	142 144 146 148	588.27 (589.1) 590.27 (590.1) 592.27 (592.1) 594.27 (594.1)	68 63 71 63	0.21 0.20 0.22 0.20	$[M+1]^+$ $[M]^+$ $[M]^+$ $[M]^+$
$[NdL^2(NO_3)_2(H_2O)_3].3H_2O$	142 146	622.27 (622.0) 626.27 (627.0)	68 52	1.17 0.89	$[M]^+$ $[M+1]^+$
$[NdL^3(NO_3)_2(H_2O)_3].3H_2O$	144 145 148	624.27 (624.1) 625.27 (625.1) 628.27 (628.1)	94 79 70	0.51 0.43 0.38	$[M]^+$ $[M]^+$ $[M]^+$
$[NdL^4(NO_3)_2(H_2O)_3].4H_2O$	145 148 150	643.27 (643.1) 646.27 (647.1) 648.27 (648.1)	76 87 73	0.34 0.39 0.33	$[M]^+$ $[M+1]^+$ $[M]^+$
$[NdL^5NO_3(H_2O)_5].2H_2O$	142 143 146 148	577.27 (578.8) 578.27 (578.8) 581.27 (582.8) 583.27 (584.8)	54 54 55 97	0.58 0.58 0.59 1.04	$[M+1]^+$ $[M]^+$ $[M+1]^+$ $[M+1]^+$
$[NdL^6(NO_3)_2(H_2O)_3].5H_2O$	142 148	657.27 (658.3) 663.27 (664.0)	55 60	0.38 0.42	$[M+1]^+$ $[M+1]^+$

TABLE 6. TGA and DTG data of the Nd^{3+} complexes of the metformin Schiff-bases.

Compound	Temp. range °C	DTG °C	Mass loss %		Process	Product	Residue % and type Found (calculated) %
			Found	Calcd.			
$HL^1(C_{11}H_{15}N_5O)$ [R]	160-293 294-422 423-600	258 351 503	19.17 30.14 30.25	19.29 30.43 30.32	Partial decomposition Ligand decomposition Final decomposition	$HN(CH_3)_2$ HN(CH=NH)2 0.13	20.1(19.96) carbonaceous material
$[NdL^1(NO_3)_2(H_2O)_3].2H_2O$	26-191 210-368 430-565	71 143 229 330 490	6.52 14.0 13.14 22.64	6.09 13.71 13.71 22.69	Dehydration Coordination sphere Coordination sphere Partial decomposition	$2H_2O$ H_2O+HNO_3 H_2O+HNO_3 $H_2O+HN(CH_3)_2+HN(CH=NH)_2$	44.0 (29.0 Nd_2O_3 +carbonaceous material)
$[NdL^2(NO_3)_2(H_2O)_3].3H_2O$	20-196 198-361 363-648	73 293 430 591	8.5 15.3 35.2	8.64 15.84 35.06	Dehydration Coordination sphere Partial decomposition	$3H_2O$ $2H_2O+HNO_3$ $H_2O+HNO_3+HN(CH_3)_2+HN(CH=NH)_2+½CO_2$	41.0 (26.94 Nd_2O_3 +carbonaceous material)
$[NdL^3(NO_3)_2(H_2O)_3].3H_2O$	35-118 118-341 341-470	73 287 410	8.8 15.2 34.72	8.64 15.84 35.06	Dehydration Coordination sphere Partial decomposition	$3H_2O$ $2H_2O+HNO_3$ $H_2O+HNO_3+HN(CH_3)_2+HN(CH=NH)_2+½CO_2$	Not complete
$[NdL^4(NO_3)_2(H_2O)_3].4H_2O$	19-203 206-389 390-661	76 272 518 609	11.5 14.7 30.0	11.2 15.4 30.65	Dehydration Coordination sphere Partial decomposition	$4H_2O$ $2H_2O+HNO_3$ $H_2O+HNO_3+HN(CH_3)_2+HN(CH=NH)_2$	43.0 (26.18 Nd_2O_3 +carbonaceous material
$[NdL^5NO_3(H_2O)_5].2H_2O$	33-222 223-311 470-525 620-670	70 298 504 645	6.75 17.54 29.06 7.44	6.21 17.08 29.33 7.59	Dehydration Coordination sphere Partial decomposition Final decomposition	$2H_2O$ $2H_2O+HNO_3$ $3H_2O+HN(CH_3)_2+HN(CH=NH)_2$ CO_2	41.0 (29.03 Nd_2O_3 + carbonaceous material
$[NdL^6(NO_3)_2(H_2O)_3].5H_2O$	18-153 153-359 361-697	72 295 462 568	13.41 24.88 33.71	13.64 24.56 33.66	Dehydration Coordination sphere Partial decomposition	$5H_2O$ $2H_2O+2HNO_3$ $H_2O+HN(CH_3)_2+HN(CH=NH)_2+2CO_2$	30.0 (25.51 Nd_2O_3 +carbonaceous material

TABLE 7. DTA data of the Nd^{3+} complexes of the metformin Schiff-bases.

Compound	Temp. rang. °C	DTA peak	ΔH J/g	Process
HL1($C_{11}H_{15}N_5O$)	160-213 253-351 507-560	195 endo. 290 exo. 531 exo.	89 -190 - 210	Melting decomposition partial Final decomposition
[$NdL^1(NO_3)_2(H_2O)_3$].$2H_2O$	35-200 260-370 400-600	73 endo 143 328 exo. 438 exo.	75 -387 72	Dehydration Coordination sphere Partial decomposition
[$NdL^2(NO_3)_2(H_2O)_3$].$3H_2O$	20-200 200-350 360-680	77 endo. 298 exo. 452 exo. 571	322 - 611 -2610	Dehydration Coordination sphere Partial decomposition
[$NdL^3(NO_3)_2(H_2O)_3$].$3H_2O$	30-120 220-350 380-500	78 endo. 292 exo. 425 exo.	174 -415 -162	Dehydration Coordination sphere Partial decomposition
[$NdL^4(NO_3)_2(H_2O)_3$].$4H_2O$	23-190 200-371 400-660	82 endo. 274 exo. 513 exo. 618	413 -532 -1590	Dehydration Coordination sphere Partial decomposition
[$NdL^5NO_3(H_2O)_5$].$2H_2O$	31-180 260-370 425-660 660-805	75 endo. 308 exo. 613 exo. 753 exo.	140 -179 -131 -57	Dehydration Coordination sphere Partial decomposition Solid state reaction
[$NdL^6(NO_3)_2(H_2O)_3$].$5H_2O$	20-150 250-380 390- 600	76 endo. 306 exo. 471 exo. 550	474 - 151 -1690	Dedydration Coordination sphere Partial decomposition

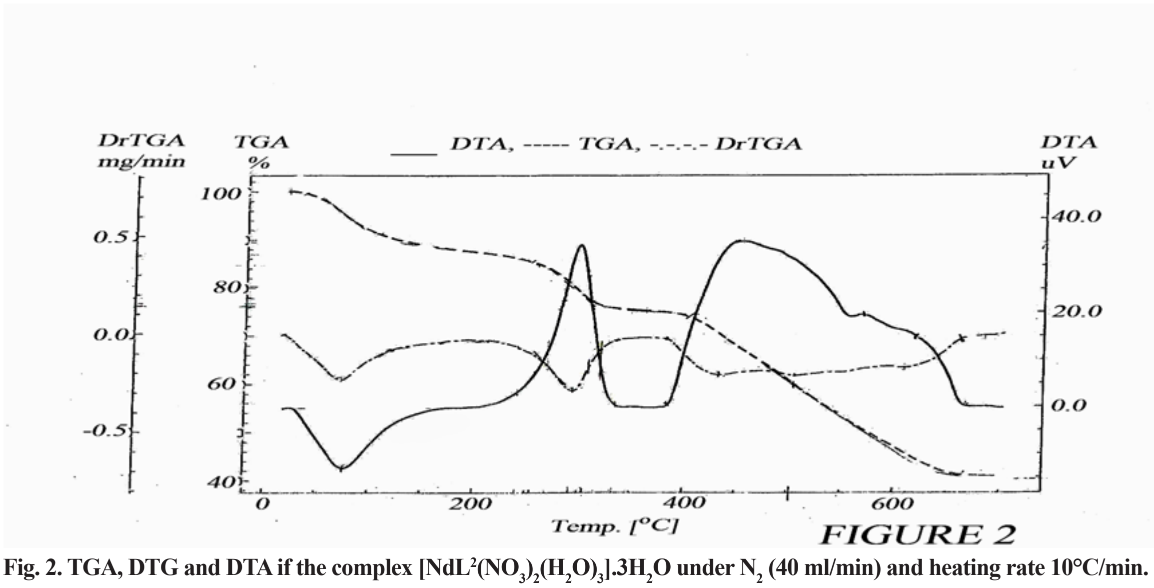

Fig. 2. TGA, DTG and DTA if the complex [$NdL^2(NO_3)_2(H_2O)_3$].$3H_2O$ under N_2 (40 ml/min) and heating rate 10°C/min.

The second step of decomposition appeared within the temperature range 210–368°C, has two DTG_{max} at 229 and 330°C corresponded to degradation of the coordination sphere through vaporization of H_2O+HNO_3 at each temperature for the complex $[NdL^1(NO_3)_2(H_2O)_3].2H_2O$. This step shows weight loss of 14.0 and 13.14% against the calculated mass of 13.71% linked with broad exothermic DTA peak extending between 260-370°C with the maximum at 328°C. The complex $[NdL^5NO_3(H_2O)_5].2H_2O$ loses also $2H_2O+HNO_3$ in the second step which occurred in the temperature period of 223-311°C with DTG_{max} at 298°C. Mass reduction observed is 17.54% (calcd. 17.08%) connected with exothermic DTA_{max} at 308°C. The second decomposition stage for the complexes $[NdL^2(NO_3)_2(H_2O)_3].3H_2O$, $[NdL^3(NO_3)_2(H_2O)_3].3H_2O$, $[NdL^4(NO_3)_2(H_2O)_3].4H_2O$ and $[NdL^6(NO_3)_2(H_2O)_3].5H_2O$ are shown in the 198-361, 118-341, 206-389 and 153-359°C range with DTG_{max} at 293, 287, 272 and 295°C, respectively. It correlates with the evolution of $2H_2O+HNO_3$ from the coordination sphere which record mass reduction of (found/calcd.): 15.3/15.84%, 15.2/15.84%, 14.7/15.4% and 24.88/24.56% linked with exothermic DTA_{max} at 298, 292, 274 and 306°C, respectively.

In the third decomposition step, evolution of the remaining co-ligands in the coordination sphere as well as oxidative degradation of the Schiff-bases takes place. The complexes $[NdL^1(NO_3)_2(H_2O)_3].2H_2O$ and $[NdL^3(NO_3)_2(H_2O)_3].3H_2O$ show this step in the 430-565 and 341-470°C range with DTG_{max} at 490 and 410°C. Mass reduction observed are 22.64 and 34.72% against the calculated mass of 22.69 and 35.06% linked with exothermic DTA_{max} at 438 and 425°C. On the other hand, the complexes $[NdL^2(NO_3)_2(H_2O)_3].3H_2O$, $[NdL^4(NO_3)_2(H_2O)_3].4H_2O$ and $[NdL^6(NO_3)_2(H_2O)_3].5H_2O$ indicated this step in the 363-648, 390-661 and 361-697°C region with DTG_{max} at 430, 591; 518, 609 and 462, 568°C, respectively. Depression of mass observed is (found/calcd.) 35.2/35.06%, 30.0/30.65 and 33.71/30.66% correlated with exothermic DTA_{max} at 452,571 ; 513, 618 and 471, 550°C, respectively. The complex $[NdL^5NO_3(H_2O)_5].2H_2O$ display the third and fourth steps in the 470-525 and 620-670°C range with DTG_{max} at 504 and 645°C which refers to the continuation of coordination sphere decomposition and oxidation of the organic ligand. Mass lowering in this step is 29.06% and 7.44% (calcd. 29.33% and 7.59%) associated with exothermic DTA_{max} at 613 and 753°C.

The decomposition of the mentioned complexes in nitrogen atmosphere leads probably to appropriate metal oxide and 4.49-16.82% carbon as final products, which is characteristic for investigations carried out in N_2 atmosphere [46]. Previous TGA analysis of HL^1 Schiff-base showed that about 20% of carbonaceous material was obtained at 750°C which enhances the obtained results [15].

Mechanism of thermal decomposition

Figure 3 shows IR spectra of the complex $[NdL^2(NO_3)_2 (H_2O)_3]. 3H_2O$ heated at 110, 370, 430 and 600 °C. It shows that the IR spectra changes shape, intensity and position of some characteristic bands. The disappearance of the broad bands at 3581 and 3438 cm^{-1} in the IR spectrum of heated complex at 110°C indicating dehydration [33]. Also, coordinated water ia observed as medium broad band at 3410 cm^{-1}. The υ(NH) band is shifted to 3217; $υ(CH)_3$ is observed at 2919 besides υ(C=N) appears as a sharp split band with maximum at 1630 and 1543 cm^{-1}. The split band with maxima at 1306,1260 cm^{-1} and medium band at 1203 cm^{-1} of heated complex at 370°C due the nitrate ion were disappeared. Newly observed bands at 1486, 1314, and 1221 cm^{-1} which refer to the presence of the second nitrate ion. Also, υ(C=N) is shifted to 1622 cm^{-1} and υ(NH) is moved to 3234 cm^{-1} while υ(OH) is shown as a broad band at 3427 cm^{-1}. $υ(CH_3)$ band at 2913 cm^{-1} disappeared indicating cleavage of the ligand at the metformin part of the Schiff-base and evolution of $NH(CH_3)_2$ species at the same temperature. IR spectrum of the complex at 450°C shows disappearance of υ(NH) at 3234 cm^{-1}, υ(C=N) at 1622 cm^{-1}, and $υ(NO_3)$ at 1486, 1314, 1221 cm^{-1}, respectively. Absence of the strong band at 1622 cm^{-1} in the spectrum of heated complex at 600 °C indicates decomposition of the υ(C=N) group. Appearance of new bands at 3431, 2934 and 1617 cm^{-1} in the IR spectrum of 600 °C heated sample assigned to υ(OH), $υ(CH_2)$ and δ(OH) of a mixture of aqua-hydroxo species and some carbonaceous material [47]. Split medium band at 1061 and 515 cm^{-1} is representing υ(Nd−O) bands characteristic for the presence of Nd_2O_3 [48]. Suggested thermal decomposition mechanism of the complex $[NdL^2(NO_3)_2(H_2O)_3].3H_2O$ is indicated below:

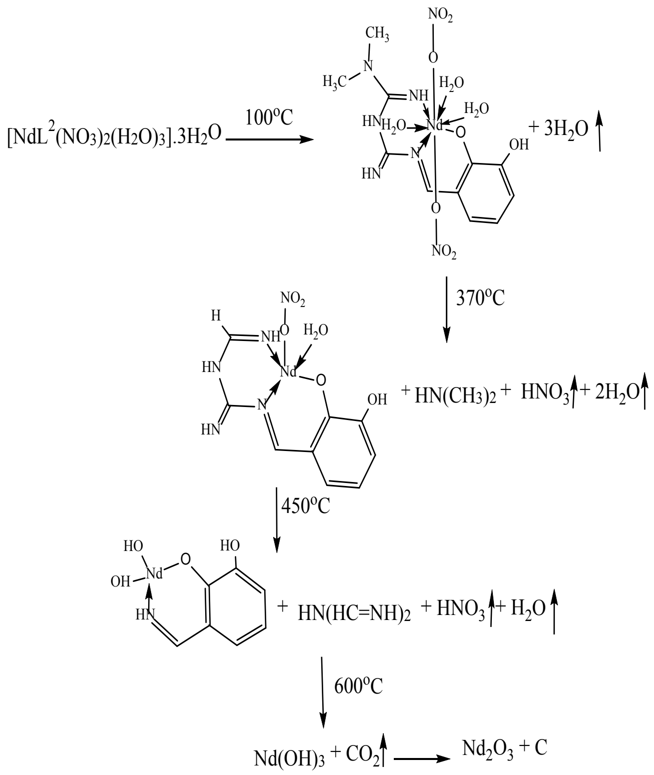

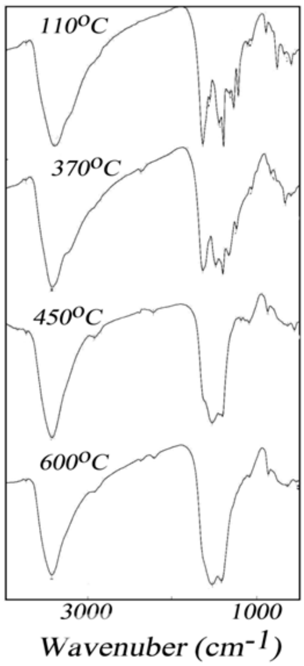

Fig. 3 IR spectra of the complex $[NdL^2(NO_3)_2(H_2O)_3].3H_2O$ at different temperature.

Kinetic and thermodynamic parameters

The kinetic parameters such as activation energy (Ea), enthalpy (ΔH), entropy (ΔS), and Gibbs free energy change of the decomposition (ΔG) are evaluated graphically by employing the Coats-Redfern method [49]. The standard equations from the transition-state theory are summarized in Table 8. The negative ΔS values indicate that the activated complexes have more ordered structure than the reactants and the reactions are slower than normal [50]. The positive values of ΔG indicate the non-spontaneous character for the reactions at the transition-state. The positive ΔH values show endothermic transition-state reactions[51].From the values of Z, the reactions of the complexes at the transition-state can be classified as a slow reaction [51].

The high values of the activation energy illustrated to the thermal stability of the complexes. The activation energies of decomposition were in the range 79-43 $kJ.mol^{-1}$. The heat of activation ΔEa , the activation enthalpies ΔH and the free energy of activation ΔG for the complex $[NdL^6(NO_3)_2(H_2O)_3].5H_2O$ is higher than that for the complex $[NdL^1(NO_3)_2(H_2O)_3].2H_2O$ (79>43, 74>38, and 166>136) which reflects the rigid structure of the Schiff-base in the first due to the presence of the phenyl ring in the Schiff-base ligand. Values of activation energy, activation enthalpy and activation free energy of the second decomposition process of the isostructureal complexes $[NdL^2(NO_3)_2(H_2O)_3].3H_2O$, $[NdL^3(NO_3)_2(H_2O)_3].3H_2O$ and $[NdL^4(NO_3)_2(H_2O)_3].4H_2O$ are: ΔEa: 49<69>40; ΔH: 44<64>35 and ΔG: 139<155>126. Increase of ΔEa , ΔH and ΔG values for the complex $[NdL^3(NO_3)2(H_2O)_2].3H_2O$ may correlate to its capability of strongly hydrogen bonding through m-OH of the H_2L^3 Schiff-base. The correlation coefficients of the Arrhenius plots of the thermal decomposition steps were found to lie in the range 0.999 to 0.978 showing a good fit with linear function.

3D molecular modeling and analysis

Since we failed to obtain single crystals for these complexes, molecular modeling studies of the representative complex $[NdL^1(NO_3)_2(H_2O)_3].2H_2O$ was carried out. All calculations were performed using CS Chem3D Pro Molecular Modeling and Analysis Program [52]. In view of the eight coordination of the Nd^{3+} complexes, the molecular modeling of the complexes is based on its hexagonal bipyramid structure. Energy minimization was repeated several times to find the global minimum [52]. All measurements of bond lengths and bond angles are given in Table 9. Results show that the coordination sphere around Nd^{3+} has the following bond lengths: Nd–O1, Nd–O15 and Nd–O16 (H_2O) are 2.316, 2.306 and 2.312 Å; Nd–O4(Schiff-base) 2.337Å; Nd–N7 and Nd-N9 (Schiff-base) are 2.373 and 2.318 Å which all form hexagon. The bond lengths inside the hexagone are in the range 2.306-2.373 Å. Nd–O17 and Nd–O23 bond lengths are 2.283 and 2.231 Å and lie on the apexes of hexagonal bipyramide stereochemistry (Structure 2).

Structure of the complexes

The eight coordinated geometries of the Nd^{3+} complexes may include hexagonal bipyramid, cube, square prism, dodecahedron, bicapped octahedron, bicapped trigonal prism, end-bicapped trigonal prism, and end-bicapped trigonal antiprism [53]. For the complex $[NdL^1(NO_3)_2(H_2O)_3].2H_2O$, the energy of each geometry was minimized and calculated using MM2 of Chem3D Ultra computer program [52] and was found to have the following values: 436.0698, 623.2961, 616.3465, 606.3751, 602.3899, 594.8797, 586.9706, and 578.5799 kcal/mol. These values show that the complex has hexagonal bipyramid stereochemistry and its structure has one Nd^{3+} at the center of hexagon surrounded by N, N, O of the Schiff-base besides O, O, O of three H_2O groups and O, O of two NO_3^- groups at the apexes (Structure 3).

Glucose sensors

Monitoring and control of a wide range of biological processes like cellular recognition, immune response, and regulation of enzymatic activity may be realized by detecting saccharides in physiologically relevant conditions [54]. The Concanavalin A (Con A) sensor developed in 1984 was the first fluorescence-based glucose sensor. Con A is a plant lectin (carbohydrate-binding protein) and a homotetramer, with each possessing a specific glucose binding site. Con A can be labeled using a fluorophore (fluorescein isothiocyanate or allophycocyanin, as the fluorescent donor) and immobilized to fine, hollow fibers. Dextran, another polysaccharide, is also labeled with a fluorophore (rodamine or malachite green, as the fluorescent receptor) in the fiber. Glucose and dextran are competing ligands of Con A in the fiber system. The combination of dextran with Con A causes fluorescence resonance energy transfer (FRET) from the fluorescence donor to the fluorescent receptor [55, 56].

TABLE 8. Kinetic and thermodynamic parameters for the second decomposition step of the Nd^{3+} complexes of the metformin Schiff-bases.

Compound	T_{max}	ΔE_a	Z*10^4	n	r	ΔH	ΔS	ΔG
$[NdL^1(NO_3)_2(H_2O)_3].2H_2O$	312	43	2.3*10^4	0.5	0.999	38	-166	136
$[NdL^2(NO_3)_2(H_2O)_3].3H_2O$	293	49	2.2*10^{*4}	0.66	0.999	44	-167	139
$[NdL^3(NO_3)_2(H_2O)_3].3H_2O$	287	69	4.3*10^4	0.66	0.995	64	-161	155
$[NdL^4(NO_3)_2(H_2O)_3].4H_2O$	272	40	2.1*10^4	0.66	0.988	35	-167	126
$[NdL^5NO_3(H_2O)_5].2H_2O$	298	57	3.0*10^4	0.66	0.978	52	-164	146
$[NdL^6(NO_3)_2(H_2O)_3].5H_2O$	295	79	3.8*10^4	2.0	0.993	74	-162	166

ΔEa, ΔH, ΔG in kJ/mol
ΔS in JK-1mol^{-1}
Z in S^{-1}

TABLE 9. Bond lengths (Å) and bond angles (°) of the complex [NdL[1](NO_3)$_2$(H_2O)$_3$].2H_2O.

Atoms	Bond lengths	Atoms	Bond angles	Atoms	Bond angles
N(27)-O(29)	1.346	C(13)-N(11)-C(12)	122.062	O(23)-Nd(8)-N(7)	49.582
N(27)-O(28)	1.345	C(13)-N(11)-C(10)	117.836	O(23)-Nd(8)-O(4)	48.768
N(24)-O(26)	1.363	C(12)-N(11)-C(10)	120.094	O(23)-Nd(8)-O(1)	175.453
N(24)-O(25)	1.325	O(29)-N(27)-O(28)	93.087	O(17)-Nd(8)-O(15)	136.927
O(23)-N(27)	2.180	O(29)-N(27)-O(23)	124.537	O(17)-Nd(8)-O(16)	100.788
C(20)-C(21)	1.339	O(28)-N(27)-O(23)	122.180	O(17)-Nd(8)-N(9)	94.983
C(19)-C(20)	1.338	O(26)-N(24)-O(25)	116.806	O(17)-Nd(8)-N(7)	70.494
C(18)-C(19)	1.341	O(26)-N(24)-O(17)	110.267	O(17)-Nd(8)-O(4)	140.094
O(17)-N(24)	1.630	O(25)-N(24)-O(17)	111.663	O(17)-Nd(8)-O(1)	64.129
N(11)-C(13)	1.486	N(14)-C(6)-N(7)	117.272	O(15)-Nd(8)-O(16)	67.039
N(11)-C(12)	1.483	N(14)-C(6)-N(5)	117.936	O(15)-Nd(8)-N(9)	89.252
N(11)-C(10)	1.279	N(7)-C(6)-N(5)	124.782	O(15)-Nd(8)-N(7)	150.069
N(9)-C(10)	1.273	C(10)-N(5)-C(6)	132.657	O(15)-Nd(8)-O(4)	74.788
Nd(8)-O(23)	2.231	N(27)-O(23)-Nd(8)	66.948	O(15)-Nd(8)-O(1)	74.081
Nd(8)-O(17)	2.283	N(24)-O(17)-Nd(8)	104.804	O(16)-Nd(8)-N(9)	156.172
O(15)-Nd(8)	2.306	N(11)-C(10)-N(9)	118.869	O(16)-Nd(8)-N(7)	128.178
O(16)-Nd(8)	2.312	N(11)-C(10)-N(5)	117.374	O(16)-Nd(8)-O(4)	65.828
Nd(8)-N(9)	2.318	N(9)-C(10)-N(5)	122.867	O(16)-Nd(8)-O(1)	62.938
N(7)-C(22)	1.360	C(22)-N(7)-Nd(8)	124.705	N(9)-Nd(8)-N(7)	73.999
N(7)-Nd(8)	2.373	C(22)-N(7)-C(6)	113.863	N(9)-Nd(8)-O(4)	111.617
C(6)-N(14)	1.270	Nd(8)-N(7)-C(6)	116.168	N(9)-Nd(8)-O(1)	109.648
C(6)-N(7)	1.277	N(7)-C(22)-C(2)	130.413	N(7)-Nd(8)-O(4)	88.319
C(10)-N(5)	1.275	C(21)-C(20)-C(19)	119.774	N(7)-Nd(8)-O(1)	134.620
N(5)-C(6)	1.273	C(20)-C(19)-C(18)	120.443	O(4)-Nd(8)-O(1)	127.063
Nd(8)-O(4)	2.337	C(10)-N(9)-Nd(8)	126.126	Nd(8)-O(4)-C(3)	120.752
C(21)-C(3)	1.346	C(20)-C(21)-C(3)	122.849	C(21)-C(3)-O(4)	115.415
C(3)-O(4)	1.594	C(19)-C(18)-C(2)	122.842	C(21)-C(3)-C(2)	117.560
C(2)-C(22)	1.458	O(23)-Nd(8)-O(17)	120.054	O(4)-C(3)-C(2)	126.942
C(2)-C(18)	1.351	O(23)-Nd(8)-O(15)	102.106	C(22)-C(2)-C(18)	115.389
C(3)-C(2)	1.456	O(23)-Nd(8)-O(16)	113.476	C(22)-C(2)-C(3)	128.100
O(1)-Nd(8)	2.316	O(23)-Nd(8)-N(9)	72.441	C(18)-C(2)-C(3)	116.511

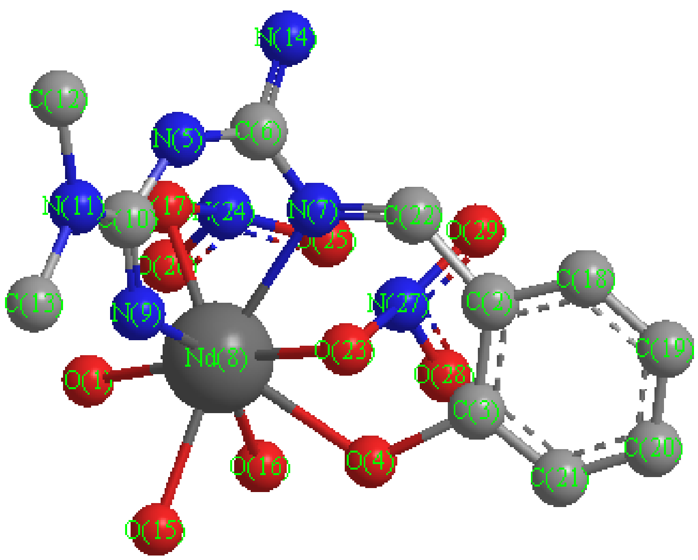

Structure 2. 3D structure of the complex [NdL[1](NO_3)$_2$(H_2O)$_3$].2H_2O.

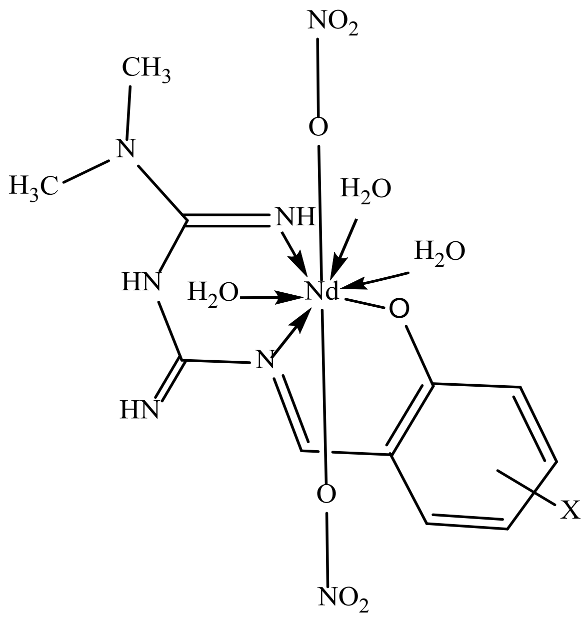

X= H , $[NdL^1(NO_3)_2(H_2O)_3].2H_2O$
X= o-OH, $[NdL^2(NO_3)_2(H_2O)_3].3H_2O$
X= m-OH, $[NdL^3(NO_3)_2(H_2O)_3].3H_2O$
X= p-OH, $[NdL^4(NO_3)_2(H_2O)_3].4H_2O$

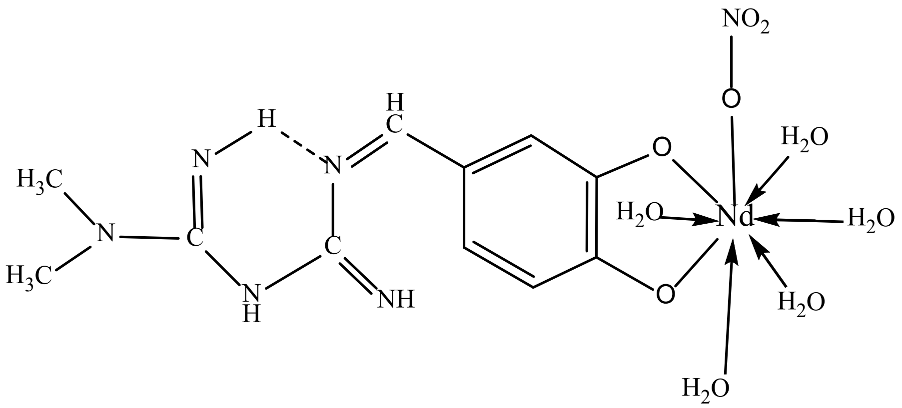

$[NdL^5(NO_3)(H_2O)_5].2H_2O$

Structure 3. Hexagonal bipyramid stereochemistry of the Nd^{3+}complexes of the metformin Schiff-bases

The earliest method for glucose detection was based on the formation of a Schiff base (imine) between aldehydes and aromatic amines. The reaction of the aldehyde group on glucose with 2-methylaniline (o-toluidine) forms a stable blue/green color imine (an anil) which absorb in the visible region at 625 nm. The main weakness of this method is its lack of selectivity owing to aldehyde being the common functional group in numerous sugars and consequent prevalence of false-positive results [54].

Another alternative method for enzyme-free glucose sensors is synthetic boronic acid-based receptors [57,58]. A boronic acid is a substituted boric acid containing a carbon (C)-boron (B) bond that belongs to the larger class of organoboranes and serves as a Lewis acid capable of reacting with Lewis bases, such as cis-1,2-diol and cis-1,3-diols or amino acids, to form reversible covalent complexes of five and six-membered cyclic boronate esters. During the last decade, numerous boronic acid-based fluorescent sensors have developed as saccharide sensors and some specific bisboronic acid sensors even reveal high selectivity for D-glucose [59-61]. Boronic acid sugar recognition can be explained by the nitrogen (N)-B interaction and the photoinduced energy transfer (PET) mechanism [61].

The incoming sugar with deprotonated hydroxyl groups can replace the coordinated water molecules in the Nd(III) complexes. This result hypothesizes that the Nd-metformin Schiff-base complexes may be useful for detecting sugars in neutral aqueous media.

Absorption characteristics of glucose-Nd complexes interaction

Interaction of 10^{-4} M of the Nd(III) complexes with glucose have been recorded in an aqueous solution of phosphate buffer of pH 7.4 using absorption spectra. The results showed that with increasing the glucose concentration from $1x10^{-4}$ M to $8x10^{-4}$ M causes moving of the complex band to the 424-333 nm signaling red shift of 14, 34 and 24 nm for the complexes $[NdL^2(NO_3)_2(H_2O)_3].3H_2O$,$[NdL^4(NO_3)_2(H_2O)_3].4H_2O$ and $[NdL^6(NO_3)_2(H_2O)_3]. 5H_2O$ as well as a blue shift of 14, 5 and 17 nm for the complexes $[NdL^1(NO_3)_2(H_2O)_3].2H_2O$,$[NdL^3(NO_3)_2(H_2O)_3].3H_2O$ and $[NdL^5NO_3(H_2O)_5].2H_2O$ associated with hyperchromism (Fig. 4 and Table 10).

Assuming the formation of a 1:1 host-guest complex, the binding constant K_b was calculated based on the following double-reciprocal relation [62]:

$$1/\Delta A = 1/\Delta\varepsilon[complex]_o + 1/K[glucose]_o \Delta\varepsilon[complex]_o$$

Where ΔA is the difference between the absorbance of complex in the presence and absence of glucose, Δε is the difference between the molar absorption coefficients of glucose and the complex. $[glucose]_o$ and $[complex]_o$ are the initial concentration of glucose and the complex. The intrinsic binding constants K_b of the complexes are in the 914-630 M^{-1} range with a correlation coefficient in the 0.966-0.990 range (Table 10).

Fluorescence spectra of glucose-Nd complexes mixture

Since most glucose sensors are fluorescent, the luminescence spectra for solutions of the free complexes and mixtures of the complexes with variable concentrations of glucose were measured. On excitation with λ=293 nm, glucose exhibit a weak fluorescence emission at λ=358 nm. Accordingly, addition of glucose ($1x10^{-4}$ M-$7x10^{-4}$ M) causes a remarkable increase of the complexes fluorescence emission from 343 to 497 nm. Also, hyperchromism and a red shift of 53 nm for the complex $[NdL^5NO_3(H_2O)_5].2H_2O$ and a blue shift of 25 nm for the complex $[NdL^2(NO_3)_2(H_2O)_3].3H_2O$ was observed (Table 10 and Fig. 5).

The binding constants of the complexes (10^{-4} M) with variable concentrations of glucose can be obtained from Benesi-Hildebrand plot, which is double reciprocal type plot of $1/(I-I_o)$ vs. 1/[glucose], where I_o and I are the fluorescence intensities in the absence (free complex) and presence of the glucose, $[glucose]_o$ is the initial concentration of glucose, and I_1 is the limiting intensity of fluorescence [62]. The binding constant (K_b) is the association constant for 1:1 complex which can be calculated from the fluorescence data based on the following equation:

$$1/(I-I_o) = 1/(I_1-I_o)K[glucose]_o + 1/I_1-I_o$$

Where I_1 is the limiting intensity of fluorescence. Thus the K_b value was obtained from the slope and the intercept of the plot. The values of binding constant of the Nd^{3+} complexes are in the range of 973-621 M^{-1} with a correlation coefficient in the 0.967-0.985 range. The obtained K_b value is in reasonable agreement with that obtained from UV-Vis absorption data.

TABLE 10. Binding constants (K_b M^{-1}) of the interaction between the Nd^{3+} complexes of the metformin Schiff base and glucose.

Compound	UV-Vis				Fluorescence			
	λ_{max}	Δλ	K_b M^{-1}	R-squared	λ_{max}	Δλ	K_b M^{-1}	R-squared
$[NdL^1(NO_3)_2(H_2O)_3].2H_2O$	383	-14	798	0.979	343	–	851	0.967
$[NdL^2(NO_3)_2(H_2O)_3].3H_2O$	406	14	882	0.982	408	-25	865	0.978
$[NdL^3(NO_3)_2(H_2O)_3].3H_2O$	333	-5	894	0.966	384	–	887	0.970
$[NdL^4(NO_3)_2(H_2O)_3].4H_2O$	371	34	714	0.994	437	–	773	0.974
$[NdL^5NO_3(H_2O)_5].2H_2O$	387	-17	630	0.971	497	53	621	0.985
$[NdL^6(NO_3)_2(H_2O)_3].5H_2O$	424	24	914	0.990	459	–	973	0.984

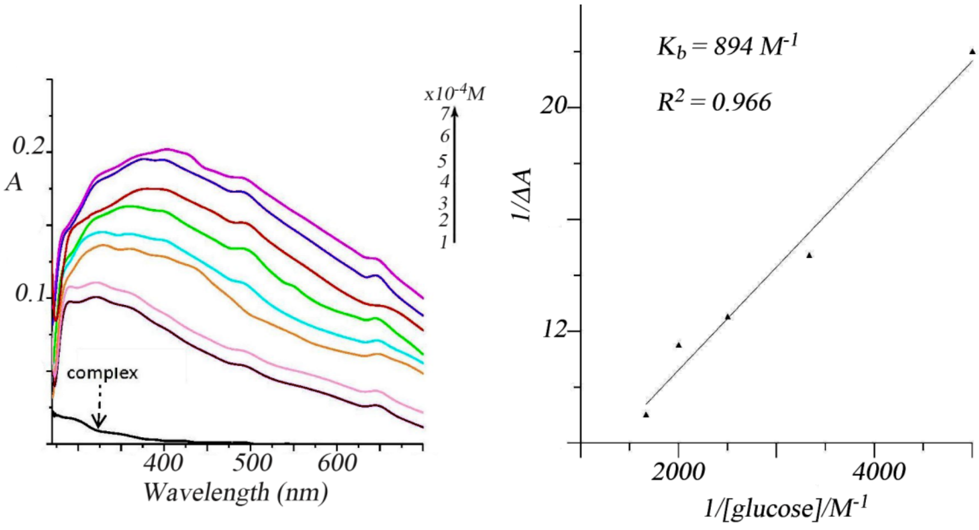

Fig. 4. UV-Vis spectra of the complex[$NdL^3(NO_3)_2(H_2O)_3$].$3H_2O$ (10^{-4} M) in presence of increasing amounts of glucose ($1x10^{-4}$ M–$7x10^{-4}$ M) using phosphate buffer (pH 7.4).

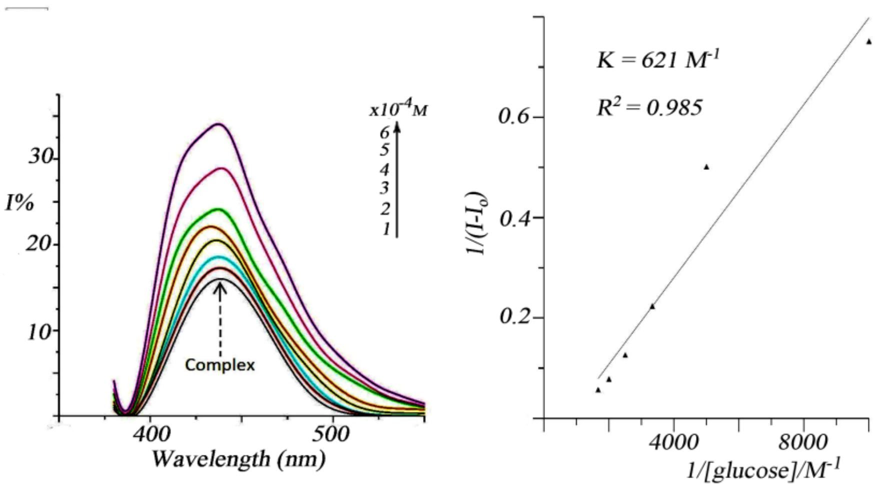

Fig. 5 Fluorescence spectra of the complex [$NdL^4(NO_3)_2(H_2O)_3$].$4H_2O$ (10^{-4} M) in presence of increasing amounts of glucose ($1x10^{-4}$ M–$7x10^{-4}$ M) using phosphate buffer (pH 7.4).

Interaction of salophene–La^{3+} with glucose, maltose and maltotriose forms complex with 1:1 stoichiometry exhibiting binding constants of 500; 1666; and 2500 M^{-1}, respectively [63]. pH-depression method was used to calculate $K_{eq\text{-}tet}$ for the glucose-PBA (phenyl boronic acid) complex (110 M^{-1}) but using the ARS method, $K_{eq\text{-}tet}$ has the value of 77 M^{-1} at pH 7.5 [64]. ^{11}B NMR technique was followed to calculate thermodynamic stability constant of the interaction of glucose with conjugate of phenylboronic acid and an La(DTPA) recording the value of 712 M^{-1} [65]. The calculated K_b values show the good binding ability of the Nd(III) complexes to glucose at pH 7.4 which can be used in diabetes management. This may be obtained through substitution of the coordinated water by glucose molecule. The highest K_b value (Table 10) obtained for the complex [$NdL^6(NO_3)_2(H_2O)_3$].$5H_2O$ (914 and 973 M^{-1}) may be due to the presence of naphthyl ring in the Shiff-base ligand of the complex. On the contrary, the relative low K_b value for the complex [$NdL^1(NO_3)_2(H_2O)_3$].$2H_2O$ (798 and 810 M^{-1}) may be due to the absence of a second o-OH group in the Schiff-base ligand which can be substituted by the glucose molecule. The K_b values for the complexes [$NdL^2(NO_3)_2(H_2O)_3$].$3H_2O$, [$NdL^3(NO_3)_2(H_2O)_3$]. $3H_2O$ and

$[NdL^4(NO_3)_2(H_2O)_3].4H_2O$ (882 < 894 > 825 M^{-1} and 865 < 887 > 860 M^{-1}) may correlate with the position of the second –OH group in the phenyl ring of the Schiff-base (o-, m- and p-substituted). The complex $[NdL^5(NO_3)(H_2O)_5].2H_2O$ has the lowest K_b value (630 and 621 M^{-1}). In this complex Nd^{3+} is strongly coordinated to two O atoms of the hydroxyl groups of the Schiff-bases which reflected in a weak bonding with the interacting glucose molecule. Fig. 6(a) and 6(b) shows the effect of the position of the OH group on the value of the association constants for the complexes of Pr^{3+}, Nd^{3+} and Dy^{3+} with MF Schiff-bases [25,26]. The figures show that:

1- K_b values increase with an increasing atomic number from Pr^{3+} to Nd^{3+} complexes (light lanthanides).

2- Pr^{3+} and Nd^{3+}complexes contain $3H_2O$ molecues in their coordination sphere while the Dy^{3+} complexes (heavy lanthanides) contain $2H_2O$. This facilitate the interaction of the complexes with glucose which lead to higher K_b values ($[PrL^1(NO_3)_2(H_2O)_3].H_2O$, $[NdL^1(NO_3)_2(H_2O)_3].2H_2O$ and $[DyL^1(NO_3)_2(H_2O)_2]2H_2O$).

3- Also, hexagonal structure of the Pr^{3+}[21] and Nd^{3+} complexes compared to pentagonal bipyramid stereochemistry for the Dy^{3+} complexes[26]may also affect the differences in K_b values.

Viscosity measurements

Relative viscosities for glucose in the presence and absence of the complexes were calculated from the relation:

$$\eta = (t-t_o)/t_o$$

Where t is the observed flow time of glucose containing solution and t_o is the flow time of phosphate buffer alone. Data are presented as $(\eta/\eta_o)^{1/3}$ versus binding ratio r (r = [complex]/[glucose]), where η is the viscosity of glucose in the presence of complex and η_o is the viscosity of glucose alone. Titration was performed by the addition of (1-8x10^{-4} M) of the complexes to a constant solution of the glucose (10^{-4} M).

The effect of glucose on the viscosity of the complexes was measured and (Fig. 7 representative example). As shown in Fig. 7, the increase in the concentration of the glucose caused an increase in the viscosity of complexes. Thus, it can be concluded that the Nd-metformin complexes, certainly, is a glucose binder [66].

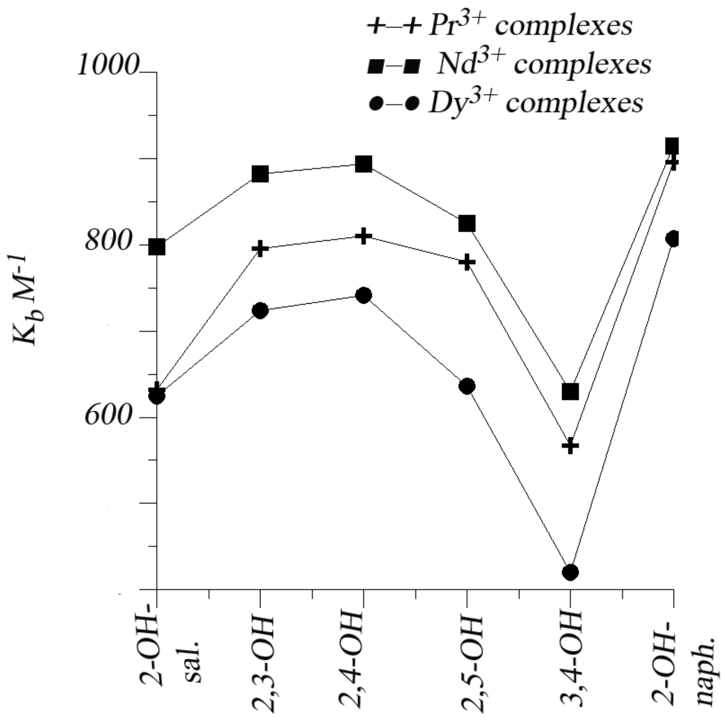

Fig. 6(a). Effect of OH position in the MF Schiff-bases of the K_b values of the Pr^{3+}, Nd^{3+} and Dy^{3+} complexes from UV-Vis spectroscopy

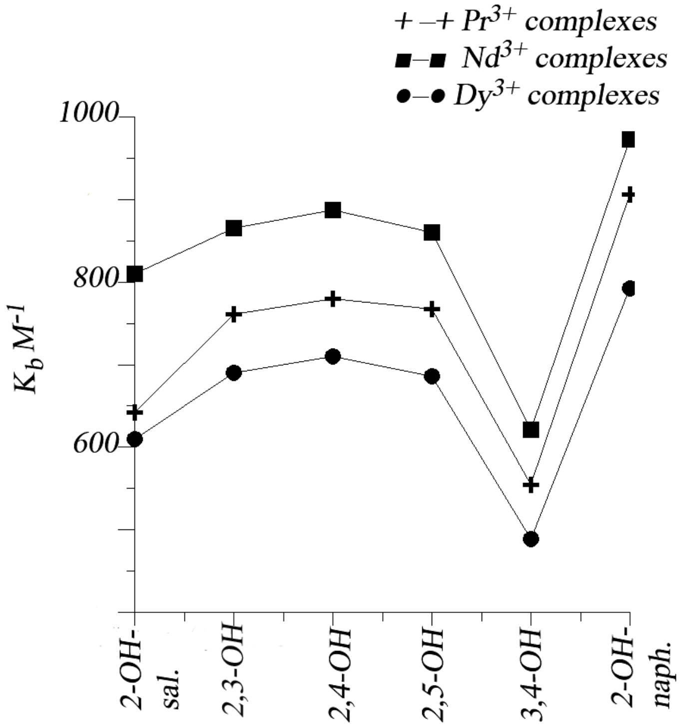

Fig. 6(b). Effect of OH position in the MF Schiff-bases of the K_b values of the Pr^{3+}, Nd^{3+} and Dy^{3+} complexes from emission spectroscopy.

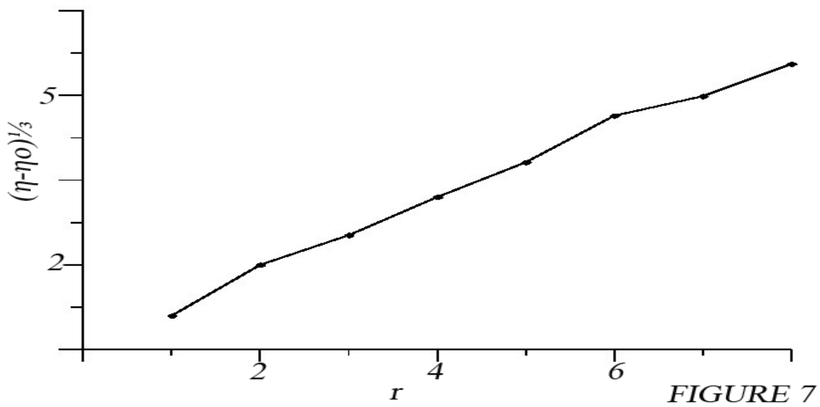

Fig. 7. Effect of increasing amounts of glucose ($1x10^{-4}$ M-$8x10^{-4}$ M) on the viscosity of the $[NdL^1(NO_3)_2(H_2O)_3].2H_2O$ complex (10^{-4}M) in phosphate buffer (pH=7.4).

Conclusion

Referring to the biological relevance of lanthanide elements and to improve the biological activity of the oral hypoglycemic agent MF, a series of Nd(III) complexes with Schiff-bases of MF with salicylaldehyde (HL^1); 2,3-dihydroxybenzaldehyde (H_2L^2); 2,4-dihydroxy-benzaldehyde (H_2L^3); 2,5-dihydroxy-benzaldehyde (H_2L^4); 3,4-dihydroxy-benzaldehyde (H_2L^5); and 2-hydroxynaphthaldehyde (HL^6) were synthesized by template reaction. Characterization of the resulting complexes was evaluated using elemental analysis, conductivity measurements, magnetic moment, spectral analysis (UV–Vis, fluorescence, IR, GC-MS, XRD), and TG, DTG and DTA. The Schiff-bases are tridentate where Nd^{3+} is bonded through –OH, azomethin C=N and C=NH (metformin) forming eight coordinated complex. On the other hand, H_2L^5 ligand is coordinated to Nd^{3+} using –OH groups -ortho to each other- on the phenyl ring of the ligand. Hexagonal bipyramid stereochemistry was suggested for the complexes based on magnetic and spectral data as well as molecular modeling calculations. Thermal properties confirm the structure of the complexes with proposed thermal decomposition mechanism. The high values of ΔE_a , ΔH, and ΔG of the complex $[NdL^6(NO_3)_2(H_2O)_3].5H_2O$ reflect the rigid structure of the Schiff-base HL^6 while those of the complex $[NdL^3(NO_3)_2(H_2O)_2].3H_2O$ may correlate to its capability of strongly hydrogen bonding through m-OH of the H_2L^3 Schiff-base. Biological activity of the complexes was evaluated by studying the interaction of these complexes with glucose in phosphate buffer solution using UV-Vis and fluorescence spectra as well as viscosity measurements. The K_b values indicate the good ability of the Nd^{3+} complexes to bind glucose in phosphate buffer medium at pH 7.4. The stereochemistry of the complexes Pr^{3+}, Nd^{3+} and Dy^{3+} and the atomic radii of the metals with the obtained K_b values and are correlated with the reactivity of the complexes towards glucose interaction.

References

1. Stepensky, D., Friedman, M., Srour, W., Raz, I., Hoffman, A. Preclinical evaluation of pharmacokinetic–pharmacodynamic rationale for oral CR metformin formulation. *J. Control Release,* **71**, 107-115 (2001).

2. Physicians. New Jersey: Desk Reference, Inc., Medical Economics Company, Vol. **57** (2003).

3. The Merck Index. Published on CD by Chapman& Hall CRC. Whitehouse Station: Merck& Co Inc, Monograph No. 6001 (1999).

4. Lu, L. P., Zhang, H. M., Feng, S. S., Zhu, M. L. Two N,N-dimethylbiguanidium salts displaying double hydrogen bonds to the counterions. *Acta Crystallogr C*. **60**(10), o740-3 (2004).

5. Dolzhenko, A. V., Kotegov, V. P., Godina, A. T., Syropiatov, B. I., Kolotova, N. V., Koz' minykh, V. O. Hypoglycemic activity of substituted amides and hydrazides of succinic acid. *Eksp. Klin. Farmakol*. **66**(3), 36-8 (2003).

6. Babykutty, P. V., Parbhakaran, P. C., Anantaraman, R., Nair, C. G. R. Electronic and infrared spectra of biguanide complexes of the 3d-transition metals. *J. Inorg. Nucl. Chem.* **36**, 3685-3688 (1974).

7. Subasinghe, S., Greenbaum, A. L., McLean, P. The insulin-mimetic action of Mn^{2+}: Involvement of cyclic nucleotides and insulin in the regulation of hepatic hexokinase and glucokinase. *Biochem. Med.* **34**, 83-92 (1985).

8. Zhu, M., Lu, L., Yang, P., Jin, X. Bis(1,1-dimethylbiguanido)copper(II) octahydrate. *Acta Crystallogr. E58:* m217-m219 (2002).

9. Patrinoiu, G., Patron, L., Carp, O., Stanica, N. Thermal behaviour of some iron(III) complexes with active therapeutically biguanides. *J. Therm. Anal. Calorim.* **72**,489-495 (2003).

10. Olar, R., Badea, M, Cristurean, E., Lazar, V., Cernat, R., Balotescu, C. Thermal behavior, spectroscopic and biological characterization of Co(II), Zn(II), Pd(II) and Pt(II) complexes with N,N-dimethylbiguanide. *J. Therm. Anal. Calorim.* **80**, 451-455 (2005).

11. Al-Saif, F. A., Refat, M. S. Synthesis, spectroscopic, and thermal investigation of transition and non-transition complexes of metformin as potential insulin-mimetic agents. *J. Therm. Anal. Calorim.* **111**, 2079- 2096 (2013).

12. El-Megharbel, S. M. Synthesis, characterization and antidiabetic activity of chromium (III) metformin complex. *J. Microb. Biochem. Technol.* **7**, 65-75 (2015).

13. Gao, J. A. A. Weak hydrolytical copper(II) complex derived from condensation of N,N-Dimethylbiguanide with 2-Pyridinecarbaldehyde synthesis, crystal structure and biological activity. *Synth. React. Inorg. Met- Org Nano-Met Chem.* **37**, 621-625 (2007).

14. Olar, R., Badea, M., Marinescu, D., Iorgulescu, E., Stoleriu, S. Ni(II) complexes with ligands resulted in condensation of N,N- dimethylbiguanide and pentane-2,4-dione. *J. Therm. Anal. Calorim.* **80**, 363-367 (2005).

15. Mahmoud, M. A., Zaitone, S. A., Ammar, A. M., Sallam, S. A. Structure and antidiabetic activity of chromium(III) complexes of metformin Schiff-bases. *J. Mol. Struct*. **1108**, 60-70 (2006).

16. Mahmoud, M. A., Zaitone, S. A., Ammar, A. M., Sallam, S. A. Synthesis, spectral, thermal and insulinenhancing properties of oxovanadium(IV) complexes of metformin Schiff-bases. *J. Therm. Anal. Calorim.* **128**, 957- 969 (2017).

17. Mahmoud, M. A., Ammar, A. M., Sallam, S. A. Synthesis, characterization and toxicity of Cu(II) complexes with metformin Schiff-bases. *J. Chinese Adv. Mat. Soc.* **5**, 75-102 (2017).

18. Taha, Z. A., Ajlouni, A. M., Al-Hassan, K. A., Hijazi, A. K., Faiq, A. B. Syntheses, characterization, biological activity and fluorescence properties of bis-(salicylaldehyde)-1,3-propylenediimine Schiff base ligand and its lanthanide complexes. *Spectrochim Acta,* **A81**, 317-323 (2011).

19. Kapoor, P., Fahmi, N., Singh, R. V. Microwave assisted synthesis, spectroscopic, electrochemical and DNA cleavage studies of lanthanide(III) complexes with coumarin based imines. *Spectrochim Acta,* **A83**, 74-81 (2011).

20. Kostova, I., Manolov, I., Momekov, G. Cytotoxic activity of new neodymium (III) complexes of bis-coumarins. *Eur. J. Med. Chem.* **39**, 765-775 (2004).

21. Łyszczek, R. Hydrothermal synthesis, thermal and luminescent investigations of lanthanide(III) coordination polymers based on the 4,4′-oxybis(benzoate) ligand. *J. Therm. Anal. Calorim*. **108**, 1101-1110 (2012).

22. Zeng, Yi-Bo., Yang, N., Liu, W.-S., Tang, N. Synthesis, characterization and DNA-binding properties of La(III) complex of chrysin. *J. Inorg. Biochem.* **97**, 258-264 (2003).

23. Wang, Z. M., Lin, H. K., Zhu, S. R., Liu, T. F., Zhou, Z. F., Chen, Y. T. Synthesis, characterization and cytotoxicity of lanthanum(III) complexes with novel 1,10-phenanthroline-2,9-bis-[agr]-amino acid conjugates. *Anticancer Drug Des.* **15**, 405-411 (2000).

24. Aime, S., Crich, S. G., Gianolio, E., Giovenzana, G. B., Tei, L., Terreno, E. High sensitivity lanthanide(III) based probes for MR-medical imaging. *Coord Chem. Rev.* **250**(11-12), 1562-1579 (2000).

25. Mahmoud, M., Abdel-Salam, E., Abou-Elmagd, M., Sallam, S. Template synthesis, spectral, thermal and glucose sensing of Pr^{3+} complexes of metformin Schiff-bases. *J. Fluoresc.* **2019**, Published online: 16 January 2019, DOI 10.1007/s10895-018-02341-5

26. Mahmoud, M. A., Abdel-Salam, E. T., Abdel Aal, N. F., Showery, Z. M., Sallam, S. A. Dy(III) complexes of metformin Schiff-bases as glucose probe: synthesis, spectral and thermal properties. *J. Coord. Chem.* **2019**, Published online: 06 February 2019, DOI .1080/00958972.2019.1569642

27. Figgis, N. B., Lewis, J. The magnetochemistry of complex compounds. In: Lewis, J., Wilkins, R. G. Interscience: New York (1960).

28. Geary, W. J. The use of conductivity measurements in organic solvents for the characterisation of coordination compounds. *Coord Chem. Rev.* **7**, 81-122 (1971).

29. Gao, J. A weak hydrolytical copper(II) complex derived from condensation of N,N-dimethylbiguanide with 2-pyridinecarbaldehyde synthesis, crystal structure and biological activity. *Synth. React Inorg Met- Org Chem Nano-Met Chem*. **37**, 621-625 (2007).

30. Nakamoto, K. Infrared and Raman spectra of Inorganic and coordination compounds: "*Applications in Coordination, Organometallic, and Bioinoraganic Chemistry*". 5th ed. Wiley: New York; (1997).

31. Kumar, D. S., Alexander, V. Macrocyclic complexes of lanthanides in identical ligand frameworks part 1. Synthesis of lanthanide(III) and yttrium(III) complexes of an 18-membered dioxatetraaza macrocycle. *Inorg. Chim. Acta,* **238**, 63-71 (1995).

32. Ankolekar, V. N., Mahale, V. B. Synthesis and Spectroscopic Investigations of Lanthanide(III) nitrate complexes with ligands obtained from 2,6-diformyl-4-methylphenol. *Synth. React. Inorg. Met- Org Chem.* **30**, 1193-1209 (2000).

33. Alaudeen, M., Prabhakaran, C. P. Synthesis and characterization of iron(III) complexes of N-(2-thienylidene)-N'-isonicotinoylhydrazine, N-(2-furylidene)-N'-salicyloylhydrazine and N-(2-thienylidene)-N'- salicyloylhydrazine. *Indian J. Chem.* **35A**, 517-519 (1996).

34. Patel, K. S., Kolawole, G. A., Earnshaw, A. Spectroscopic and magnetic properties of Schiff base complexes of oxovanadium(IV) derived from 3- methoxysalicylaldehyde and aliphatic diamines. *J. Inorg. Nucl. Chem.* **43**, 3107-3112 (1981).

35. Pearson, R. G. Hard and soft acids and bases. *J. Am. Chem. Soc*. **85**, 3353- 3539 (1963).

36. Carlin, R. L. "*Magnetochemistry*". Springer-Verlag: Berlin-Heidelberg (1986).

37. Huidrom, B., Devi, N. R., Singh, Th. D., Singh, N. R. Studies on the complexation of neodymium(III) ion with 1,2,4-1H-triazole and 1,2,3- benzotriazole in absence and presence of calcium(II) ion in aqueous and some selected different aquated organic solvents by

an absorption spectroscopy involving 4f–4f transitions. *Spectrochim Acta,* **A85**, 127-133 (2012).

38. Caires, F. J., Gigante, A. C., Gomes, D. J. C., Treu-Filho, O., Ionashiro, M. Studies on the complexation of neodymium(III) ion with 1,2,4-1H-triazole and 1,2,3-benzotriazole in absence and presence of calcium(II) ion in aqueous and some selected different aquated organic solvents by an absorption spectroscopy involving 4f–4f transitions. *Thermochim Acta,* **569**, 8-16 (2013).

39. Mehta, J. P., Bhatt, P. N., Misra, S. N. Pr(III) and Nd (III) Absorption Spectroscopic Probe to Investigate Interaction with Lysozyme (HEW). *J. Rare Earths*. **24**, 648-652 (2006).

40. Gopalakrishnan, K., Kuttappan, M., Kuppanagounder, P. E. Synthesis, spectroscopic characterization and antibacterial activity of lanthanide– tetracycline complexes. T*rans. Met. Chem*. **29**, 86-90 (2004).

41. Karraker, D. G. Hypersensitive transitions of six-, seven-, and eight- coordinate neodymium, holmium, and erbium chelates. *Inorg. Chem.* **6**, 1863-1868 (1967).

42. Henrie, D. E., Choppin, G. R. Environmental effects on f–f transitions. II. "Hypersensitivity" in some complexes of trivalent neodymium. *J. Chem. Phys*. **49**, 477-481 (1968).

43. Sinha, S. P. Spectroscopic investigations of some neodymium complexes. *Spectrochim. Acta,* **22**, 57-62 (1966).

44. Ain, Q., Pandey, S. K., Pandey, O. P., Sengupta, S. K. Synthesis, structural characterization and biological studies of neodymium(III) and samarium(III) complexes with mercaptotriazole Schiff bases. *Appl. Organometal. Chem*. **30**, 102-108 (2016).

45. Rijulal, G., Indrasenan, P. Synthesis and Characterization of Some Lanthanide(III) Complexes with 4-[N-(2-methoxybenzylimine) formyl]-2, 3-dimethyl-1-phenyl-3-pyazolin-5-one. *J. Rare Earths*. **25**, 670-673 (2007).

46. Yan, B., Zhang, H. J., Zhou, G. L., Ni, J. Z. Different thermal decomposition process of lanthanide complexes with -phenylanthranilic acid in air and nitrogen atmosphere. *Chem. Pap*. **57**, 83-86 (2003).

47. Carp, O., Gingasu, D., Mindru, I., Patron, L. Thermal decomposition of some copper–iron polynuclear coordination compounds containing glycine as ligand, precursors of copper ferrite. *Thermochim. Acta,* **449**, 55- 60 (2006).

48. Nyquist, R. A., Kagel, R. O. "*Infrared Spectra of Inorganic Compounds*". Academic Press: New York (1971).

49. Coats, A. W., Redfern, J. P. *Nature,* **201**, 68 (1964).

50. Hamada M. M., Shallaby, A. H. M., El-Shafai, O., El-Asmy, A. A. *Trans. Met. Chem*. **31**, 522 (2006).

51. Donia, A. M., Al-Ansi, T. Y., Othman, M. Q. *J. Thermal. Anal*. **5**, 857 (1997).

52. CS Chem3D Pro, version 5, CambridgeSoft Corporation, www.cambridgesoft.com. (1999).

53. Wells, A. F. "*Structural Inorganic Chemistry*". 5th ed. Oxford University Press: Oxford. ISBN 0-19-855370-6 (1984).

54. Wu ,T., Průša, J., Kessler, J., Dračínský, M., Valenta, J., Bouř, P. Detection of sugars via chirality induced in Europium(III) compounds. *Anal. Chem.* **88**, 8878-8885 (2016).

55. Oliver, N. S., Toumazou, C., Cass, A. E., Johnston, D. G. Glucose sensors: a review of current and emerging technology. *Diabet Med.* **26**, 197-210 (2009).

56. Pickup, J. C., Hussain, F., Evans, N. D., Rolinski, O. J., Birch, D. J. Fluorescence-based glucose sensors. *Biosens. Bioelectron.* **20**, 2555-2565 (2005).

57. Phillips, M. D., James, T. D. Boronic acid based modular fluorescent sensors for glucose. *J. Fluoresc*. **14**, 549-559 (2004).

58. Larkin, J. D., Frimat, K. A., Fyles, T. M., Flower, S. E., James, T. D. Boronic acid based photoinduced electron transfer (PET) fluorescence sensors for saccharides. *New J. Chem.* **34**, 2922-2931 (2010).

59. Cao, H., Heagy, M. D. Fluorescent chemosensors for carbohydrates: a decade's worth of bright spies for saccharides in review. *J. Fluoresc*. **14**, 569-584 (2004).

60. Phillips, M. D. Synthetic strategies in the design and construction of saccharide selective fluorescent sensors. *Ph.D. Thesis*. Bath: University of Bath, 2005.

61. Nishiyabu, R., Kubo, Y., James, T. D, Fossey, J. S. Boronic acid building blocks: tools for sensing

and separation. *Chem. Commun.* **47**, 1106-1123 (2011).

62. Benesi, H. A., Hildebrand, J. H. A spectrophotometric investigation of the interaction of iodine with aromatic hydrocarbons. *J. Am. Chem. Soc.* **71**, 2703-2707 (1949).

63. Lu, Y., Deng, G., Miao, F., Li, Z. Metal ion interactions with sugars. The crystal structure and FT-IR study of the $NdCl_3$–ribose complex. *Carbohydr. Res.* **338**, 2913-2919 (2003).

64. Springsteen, G., Wang, B. A detailed examination of boronic acid–diol complexation. *Tetrahedron.* **58**, 5291-5300 (2002).

65. Sun, Y., Bi, S., Song, D., Qiao, C., Mu, D., Zhang, H. Study on the interaction mechanism between DNA and the main active components in *Scutellaria baicalensis* Georgi. *Sens Actuators B: Chem.* **129**, 799- 810 (2008).

66. Hong, T., Iwashita, K., Shiraki, K. Viscosity control of protein solution by small solutes: a review. *Current Protein and Peptide Science,* **19**, 746-758 (2018).